Department of Physical Geography

Stockholm University

Impact of irrigation development and climate change on the water level of Lake Urmia, Iran

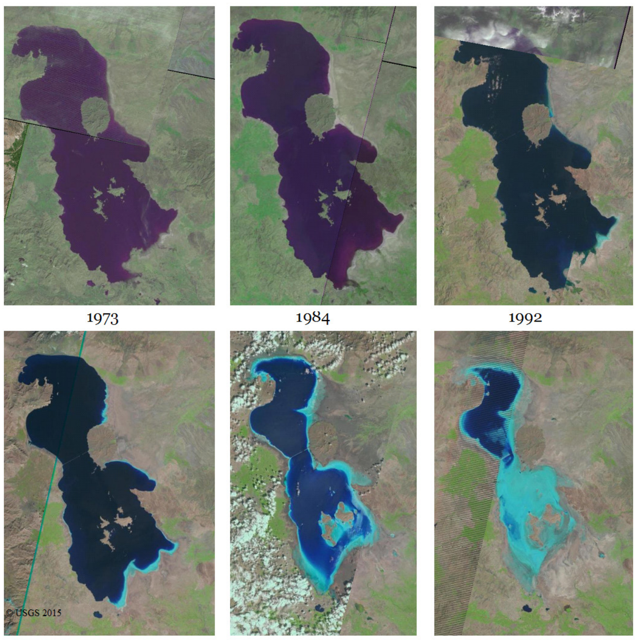

Heydar Beygi

Master's thesis
Physical Geography and Quaternary Geology, 45 Credits

NKA 118
2015

Department of Physical Geography

Stockholm University

Preface

This Master's thesis is Heydar Beygi's degree project in Physical Geography and Quaternary Geology at the Department of Physical Geography, Stockholm University. The Master's thesis comprises 45 credits (one and a half term of full-time studies).

Supervisor has been Jerker Jarsjö at the Department of Physical Geography, Stockholm University. Examiner has been Andrew Frampton at the Department of Physical Geography, Stockholm University.

The author is responsible for the contents of this thesis.

Stockholm, 11 June 2015

Steffen Holzkämper
Director of studies

Abstract

Lake Urmia, located in the north-west of Iran, is one of the largest hypersaline lakes in the world. In recent years, there has been a significant decrease in the lake's area and volume by 88% and 80% respectively. An integrated water balance model of the Lake Urmia Drainage Basin (LUDB) and Lake Urmia was developed to identify these main drivers of the significant changes, and to investigate the possible future evolution of the lake under effects of projected climate change and land use change. We used an energy balance method to estimate the evaporation from the lake and the Turc-Langbein method to estimate the evapotranspiration from the drainage basin of the lake. Agricultural irrigation water was introduced to the model as an extra precipitation over the irrigated fields, after being subtracted from the surplus runoff (precipitation−evapotranspiration). The agricultural land development was assumed to be linear that changed from 300000 ha at 1979 to 500000 at 2010, which is consistent with the best available data on the actual irrigation development in the basin. We estimated the annual evaporation over the Lake Urmia and the evapotranspiration over its drainage basin as 932 mm and 287 mm respectively. Our results showed that decreased precipitation and increased temperature over the basin since 1995 could explain 68% of the observed lake level decrease. Irrigation developments during the last four decades were found to be responsible for 32% of the observed lake level decrease. Thus the future lake level of the Lake Urmia is very likely to continue to decrease unless the current climate condition will be followed by a period of increased precipitation. If the current climate conditions will prevail also in the future, even a 20% decrease in the irrigated land area, which is actually quite ambitious, will not make the lake recover to its ecological level at the end of 2020

Key words: Lake Urmia, irrigation, Land use change, climate change, evaporation

Acknowledgement

I would like to give my sincere thanks to my supervisor Dr. Jerker Jarsjö, associate professor and senior lecturer at the Department of Physical Geography, Stockholm University, for his great support and supervision through this work.

I would like to also thank my family specially my wife who has supported me during my studies.

Contests

List of Abbreviations

LUDB	Lake Urmia Drainage Basin
CWR	Crop Water Requirement
EARWA	Eest Azarbayjan Regional Water Authority
ET	Evapotranspiration
IR	Irrigation Requirement
IRIMO	Iran's Meteorological Organization
IWR	Iranian Water Resources Management Company
MODIS	Moderate Resolution Imaging Spectroradiometer
ULRP	Urmia Lake Restoration Program
UNEP	United Nations Environment Programme
WARWA	West Azarbayjan Regional Water Authority
WL	Water Level
WST	Water Surface Temperature

1. Introduction

1.1 General

Lakes function as valuable resources for humans and can support biodiversity. Terminal lakes are, in most of the cases, a final destination for dissolved and particulate substances transported from the surrounding drainage basin. They can therefore sensitively indicate the effect of natural or human induced disturbance in their environment (Waiser and Robarts, 2009).

Saline lakes are relatively common in arid and semi-arid climate zones. Despite their importance, they have historically recived less attention than fresh water lakes (Waiser and Robarts, 2009).

Lake Urmia is one of the largest hypersaline lakes in the world and the largest in Middle East. It is located in the north-west of Iran (figure 1-1). The lake is home to a unique brine shrimp species, Artemia urmiana. Along with surrounding wetlands the lake was declared a Wetland of International Importance by the Ramsar Convention in 1971 and designated a UNESCO Biosphere Reserve in 1976 (UNEP, 2012; Ramsar 2014). The Lake is shallow with a maximum depth of 16 m and with numerous small islands (Ghaheri, et al. 1999; Ramsar 2014; Abatzopoulos et al 2006). Wetlands and brackish marshes surrounding the lake are an important place for large breeding colonies of various water birds and staging area for migratory water birds (Ramsar 2014). Surrounded by a range of high mountains, Lake Urmia Drainage Basin (LUDB) is an endorheic catchment. It is located in the relatively highly populated part of the country with population density of 70-170 persons per km^2 (figure 1-1 and figure 1-2). Furthermore, LUDB is an important agricultural region (UNEP, 2012; Abbaspour et al. 2012).

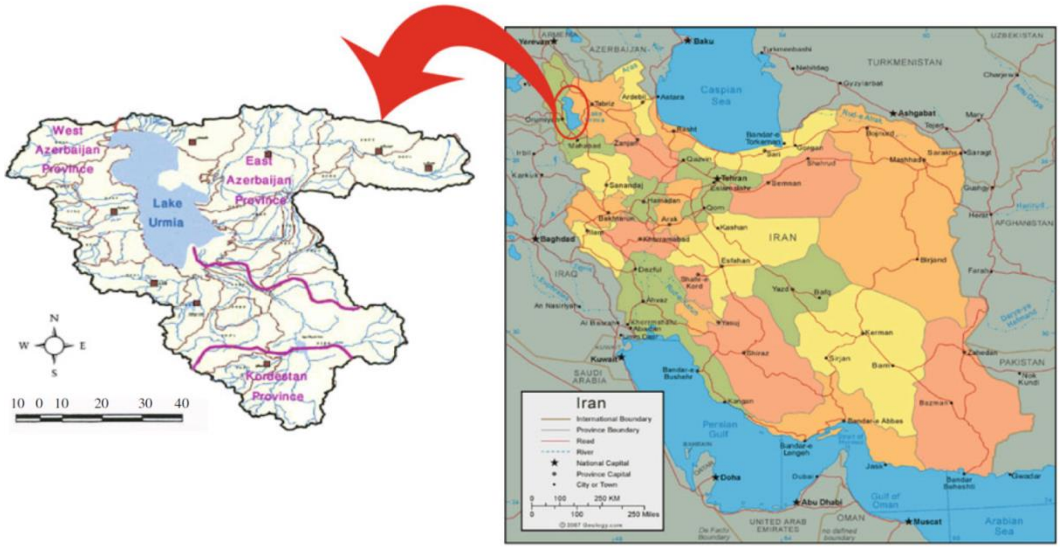

Figure 1-1. Lake Urmia drainage basin in the north west of Iran (Abbaspour et al. 2012)

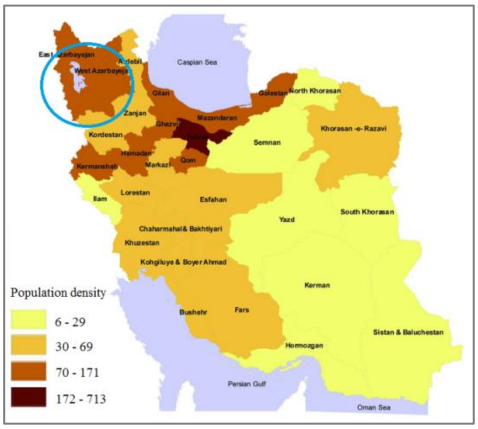

Figure 1-2. Population density of Iran and location of LUDB (UNFPA 2014)

In the last decade there has been a significant decrease in Lake Urmia's average water level (WL) by 7 m (Hassanzadeh et al., 2012; Abbaspour et al. 2012; Sima et al. 2013; UNEP, 2012), which has resulted in a dramatic shrinkage of the lake's surface area (figure 1-3 and figure 1-4), leaving behind a vast area of sodium chloride-covered salt flats (UNEP, 2012; Aghakouchak et al. 2014). In a recent study based on historical satellite images of the lake, Aghakouchak et al. (2014) reported an 88% and 80% decrease in the Lake Urmia's surface and volume respectively during the period of 1971-2014. Thus there is a great concern regarding total dry up of the lake which would destroy the ecosystem of the lake and could result in salty dust storms (UNEP, 2012; Aghakouchak et al. 2014).

Abbaspour and Nazaridoust (2007) determined the minimum water level of the Lake Urmia in which salinity of the lake remains at a tolerable level for the only remaining marine species of the lake, namely a shrimp species called Artemia urmiana. They claimed if the water level of the lake remains greater than 1274.1 m above the sea level the ecosystem of the lake and its surrounding wetlands would function sustainably. Thus current WL, 1270.59 m (at 2014), is below the ecological WL by 3.5 m in which the ecosystem of the lake is already in a great danger.

Hassanzadeh et al. (2011) investigated the main causes of the shrinkage of Lake Urmia. They concluded that the decrease of the inflow to the lake was a main factor, explaining 65% of the observed lake level decrease. Furthermore, they found that construction of four new dams and an observed decrease in precipitation over the lake surface were the next important factors, explaining 25% and 10% of the lake's declination, respectively. Using a hydrodynamic model, Abbaspour et al. (2012) concluded that if very dry conditions continue, Lake Urmia will dry up in the next ten years. Based on their study, Lake Urmia is highly sensitive to inflow from rivers to the lake. Therefore the water development projects can have a great effect on the lake's level.

While the water level of the Lake Urmia decreased significantly, this has not happened for the closest neighboring Lake with closed basin, Lake Van (Figure 1-5), located in eastern Turkey. Water level data of Lake Van extracted from previous studies (Aksoy et al. (2013) and Altunkaynak (2007)) show that lake level changes for the two lakes were similar during the historical period 1965 to 1995 (Figure 1-6). This general similarity in the two lake's historical water level behavior may in fact reflect a general similarity in the functioning of the basins and their climate conditions. The post-1995 divergent of behavior of the two lakes may hence be the results of anthropogenic changes in the Urmia Lake drainage basin (figure 1-3 and figure 1-6).

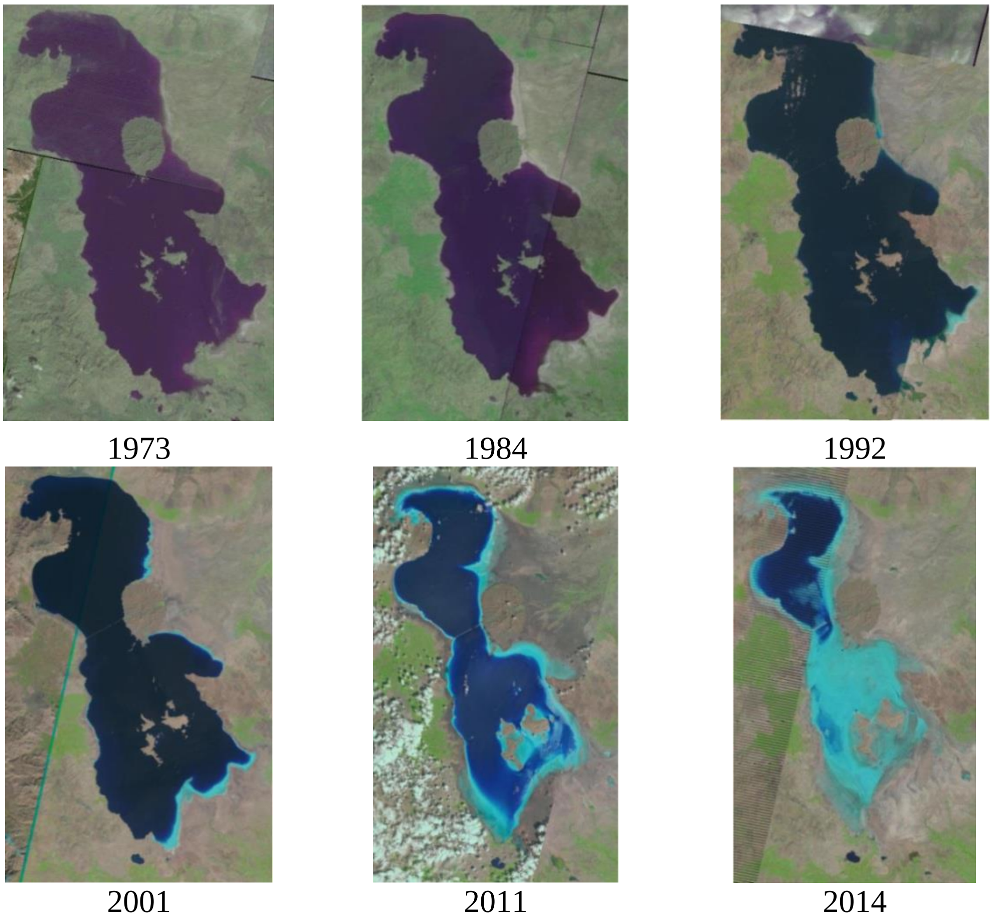

Figure 1-3. Changes in the surface area of Lake Urmia from August 1973 to August 2014, derived from LandSat imagery (USGS 2015)

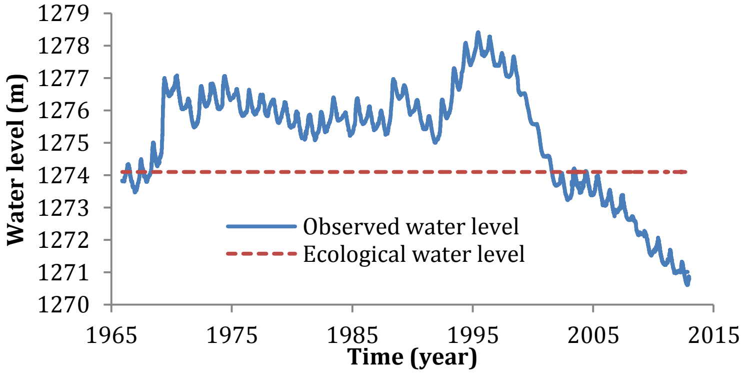

Figure 1-4. Observed and ecological water level of Lake Urmia above sea level (m)

Figure 1-5. Relative position of Lake Urmia and Lake Van (NASA 2015)

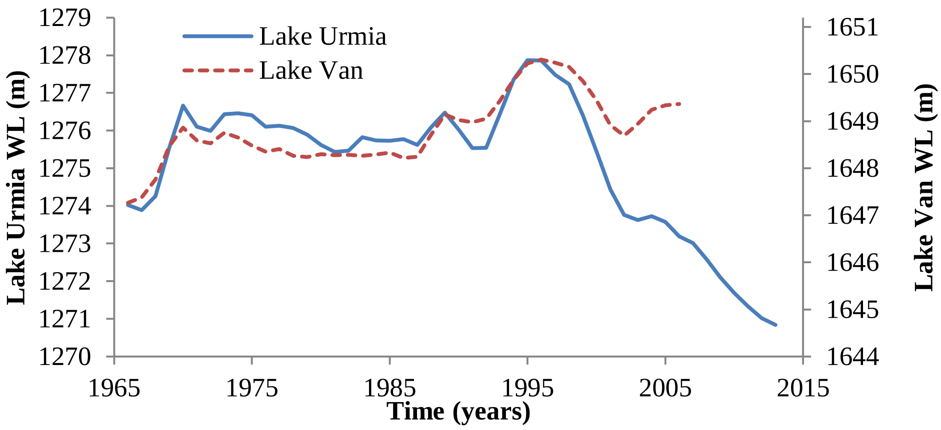

Figure 1-6. Average annual water level at Lake Urmia and Lake Van

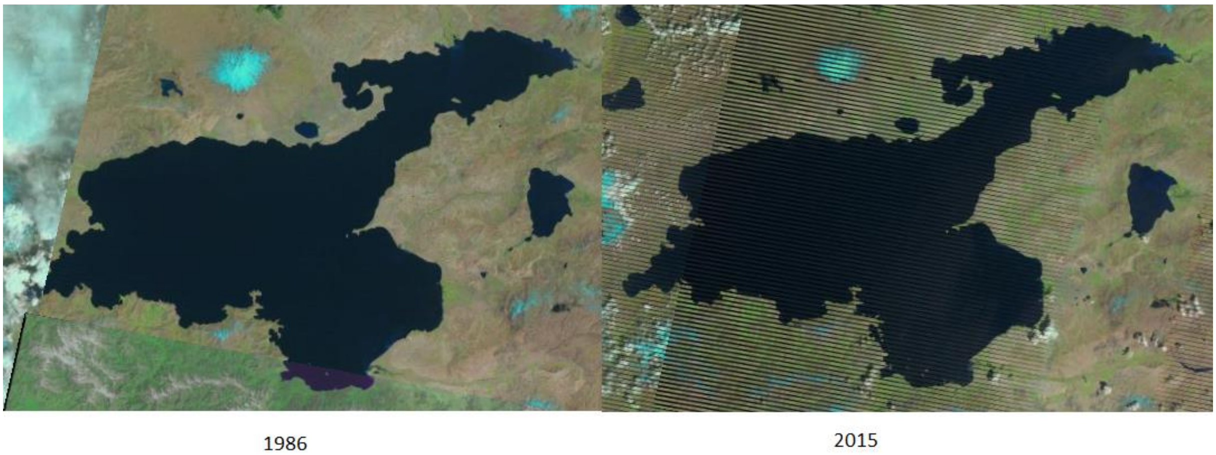

Figure 1-7. Comparison of surface area of Lake Van during the period 1986 to 2015 derived from LandSat imagery (USGS 2015)

In most of the previous studies of Lake Urmia, the main focus of the studies is the Lake itself while the lake's drainage basin has been either partly or completely ignored. In other words the lake's response to observed changes in precipitation over the lake and measured river inflow to the lake has been studied. But the effect on the river discharge into the lake of main factors such as climate conditions and land use changes in the lake's drainage basin has not been studied. Furthermore, only surface water flows have been considered as inflow to the lake (Hassanzadeh et al. 2011; Abbaspour et al. 2012; Aghakouchak et al. 2014). The aim of this study is to develop an integrated water balance model of the LUDB and Lake Urmia and apply it to study impacts of historical land use change and climate change on lake level and lake volume. We furthermore aim at investigating the possible future evolution of the lake under the effect of projected climate change and different conceivable water resource management plans.

1.2 Study area

Lake Urmia, located in north-west Iran (37º30', N, 46 º 00' E,), is the largest in Middle East and world's sixth largest saline lake with a surface area of approximately 4750-6000 km^2 Extending 140 km and 85 km in south-north and east-west direction respectively during the historical period between 1965 and 2000 (Ghaheri, et al. 1999; Abbaspour et al. 2012; UNEP, 2012; Abatzopoulos et al 2006; Waiser and Robarts, 2009). Lake Urmia's drainage basin has an area of 51876 km^2 including the lake. It is divided between three provinces, West Azerbaijan, East Azerbaijan and Kordestan. Under normal conditions during the historical period, the water level of the lake covered approximately 10% of the catchment area. The basin is located in the relatively highly populated part of the country (figure 1-2) with great fertile agricultural lands. The lake is located at an altitude of 1250 m above sea level with an average and a maximum depth of 6 m and 16 m respectively (Abatzopoulos et al 2006). The lake's total annual inflow of 6.900 km^3 has been estimated to be supplied from rivers by 4.9 km^3, flood waters by 0.5 km^3 and direct precipitation over the lake by 1.5 km^3 (Ghaheri, et al. 1999; Eimanifar and Mohebbi, 2007). The main rivers of the LUDB are given in table (1-1). The only known outfput from the lake however, is direct evaporation from the lake surface (Hassanzadeh et al. 2011)

Table 1-1. Main river inflows to Lake Urmia (Ghaheri, et al. 1999)

River	Length (km)	Average flow (m^3/s)	Sub-basin area (km^2)
Zarinneb Rood	230	45.8	11897
Simineh Rood	145	9.5	3656
Barandoozchai	70	8.3	1318
Nazloochai	85	7.87	2267
Mahabad Chai	80	6.5	1528
Shahrichai	70	5.33	720
Rowzehchai	50	1.33	453
Godarchai	100	0.34	2123
Zoolachai	84	-	2090

Lake Urmia with a salinity between 166 and 340 g/l in the past 41 years can be classified as a hypersaline lake (Karbassi, et al., 2010; Waiser & Robarts, 2009). The average concentration of different substances in Lake Urmia measured in 2008, including the average salinity and total dissolved solids is given in table 1-2. Due to the recent decrease in the lake's volume, the lake's salinity has increased dramatically, which can threat the lake's only habitant, a brine shrimp, Artemia urmiana. This will disturb the whole simple pyramid ecosystem of the lake's ecological zone, since there is no substitute for the Artemia as an energy supplier, in the lowest level of the food chain of the ecosystem (Abbaspour and Nazaridoust 2007).

The main human induced disturbances on the lake and its basin are the construction of a 15 km long causeway over the lake splitting the lake in two parts with only one opening of 1.25 km, and excessive agricultural land expansion along with dam constructions in the main rivers that flow into the lake (Ghaheri, et al. 1999, Abbaspour et al. 2012, UNEP, 2012).

Table 1-2. Average concentration of the different substances in the Lake Urmia in year 2008 (Karbassi, et al., 2010)

Substance (g/l)	Average concentration (g/l)
Cl	216
Na	125
SO_4	22.4
Mg	11.3
K	2.63
HCO_3	1.38
Ca	0.553
Salinity	339
Total Dissolved Solids	380

Zeinoddini et al., (2009) made simulations of the effect of the causeway on the flow and salinity regimes of the Lake Urmia using commercially available MIKE hydrodynamic models (i.e. MIKE 21 and MIKE 3). They defined several hypothetical scenarios including current condition with existing causeway; total removal of the causeway; and increasing the opening of the causeway up to 4.2 km. They concluded that the causeway does not have a significant effect on the salinity regime in the north and south part of the lake.

According to Iranian Water Resources Management Company (IWR) there are in total 104 dams in LUDB of which 56 are operating, 9 are under construction, and 39 are under study. Table 1-3 presents a brief description of the dams in the basin (IWR, 2014). The location of the main rivers and dams are shown in figure 1-8. Figure 1-9 indicate the total regulating volume of the constructed dams on the rivers in Lake Urmia's basin in the past years. The majority of the dam constructions were completed in the past three decades. The total dam volume in the basin has doubled in the past three decades (Iranian Water Resources Management Company 2014).

Most of the water regulated by dams is used for irrigation. The data of aquastat from FAO (2014) independently show that 92% of all water withdrawals in Iran are consumed in the agriculture sectors. But unfortunately, there is no freely available statistical data for agriculture for the considered region. Some agricultural data however, was provided by the Urmia Lake Restoration Program (ULRP) committee located at Sharif University, Tehran after personal request (Table 1-4).

Table 1-3. Overall properties of the dams in the LUDB (IWR, 2014)

Dam condition	Number of dams	Storage volume (km^3)	Regulation volume (km^3)	Capacity for domestic and industrial water use (km^3)	Capacity for agriculture water use (km^3)	Capacity for land irrigation (ha)
Operating	56	1.763	2.060	0.389	1.320	192648
Under construction	9	1.232	1.367	0.131	1.089	173240
Under study	39	0.595	0.521	0.010	0.426	83356

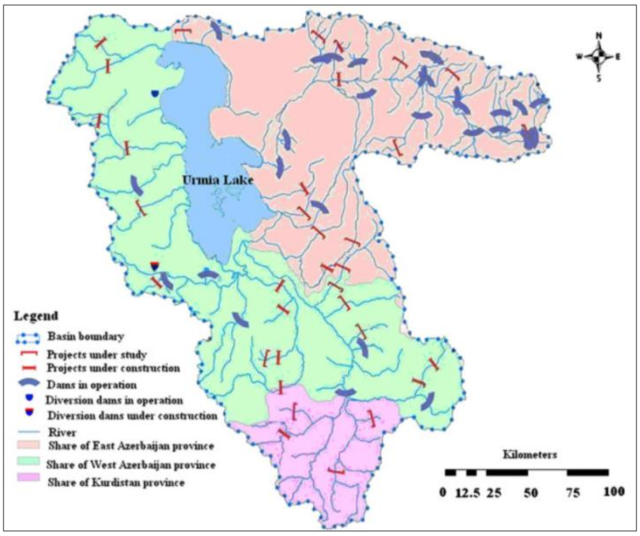

Figure 1-8. Main rivers and dams in Lake Urmia drainage basin (Hassanzadeh, et al., 2011)

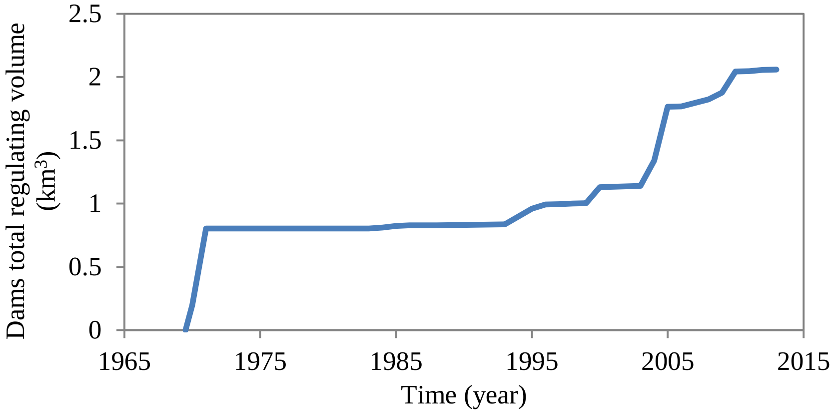

Figure 1-9. Dam construction in the Lake Urmia drainage basin (IWR, 2014)

Table 1-4. Irrigated agricultural land use in the three provinces of the Lake Urmia Drainage Basin in hectares (ULRP 2014)

Land use	East Azarbayjan	West Azarbayjan	Kurdestan	sum
Orchard	73670	93925	8208	175803
Agriculture	180856	134898	28782	344536
sum	254526	228823	36990	520339

There are no comprehensive studies on land use change in the basin, except for some regions of it. In the ULRP's website however, it is mentioned that the irrigated lands has increased from 300000 (ha) to 500000 (ha) during the last three decades (ULRP 2014). A report by Iran's ministry of agriculture based on historical satellite images (Table 1-5), indicate 11% increase in the total agricultural land and orchard in the ecological zone of Lake Urmia during the ten years period of 1990-2000 (Nasiri 2003). As presented in table 1-5 there has been a 57% increase in mixed agriculture and orchard.

Table 1-5. Land use change in the Lake Urmia's ecological zone (Nasiri A 2003)

Land use	Land use area (ha)		Land use expansion (%)
	1990	2000	
Agriculture	116866.01	128220.72	9.7
Orchard and tee sets	46065.27	47421.74	2.9
Mixed Agriculture and Orchard	14728.21	23142.21	57.1
sum	177659.5	198784.7	11.9

2. Materials and methods

2.1. Topographic and spatial data

To model the lake water level, topographic and meteorological data of LUDB was used. The SRTM 90 m digital elevation data, originally produced by NASA, and provided by the Consortium for Spatial Information (CGIAR-CSI), which have the resolution of 90m at the equator and 5deg×5deg in other places, was used to derive the Lake Urmia's drainage basin (Jarvis et al. 2008).

The Volume-Elevation and Surface Area – elevation relations of the lake and water surface temperature (WST) were taken from from results of previous studies (Sima and Tajrishy 2013).

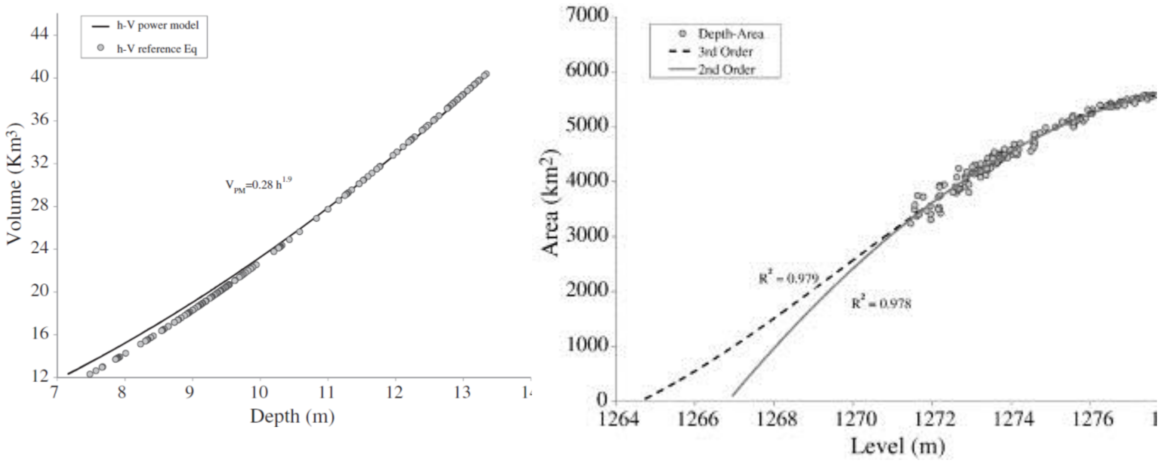

Figure 2-1. Volume-Depth and Area – Elevation relations of Lake Urmia (Sima and Tajrishy 2013)

The data of dams in the LUDB i.e. their volume and their date of starting operation is available at the Iran Water Resource Company's website (IWR, 2014).

Current total area of irrigated agricultural land use in the basin (Table 1-4) was provided by Urmia Lake Restoration Program (ULRP) committee. Nasisri (2003) studied the development and land use change in the Lake Urmia's ecological zone (Table 1-5).

2.2. Hydro-meteorological data

Monthly meteorological data (i.e. precipitation, temperature, sunshine hours, and relative humidity) was available at the Iran's Meteorological Organization (IRIMO) for the period of 1951-2010 with some minor data gaps. For some stations however, only five years of the data was available. Data series of sixteen different synoptic weather stations was selected based on the Theissen polygons, inside and outside of the LUDB (Figure 4-1). Monthly pan evaporation data and time series of mean annual water level (WL) data was provided directly by West Azarbayjan Regional Water Authority (WARWA).

All the meteorological data available for the study region, i.e. precipitation, temperature, sunshine hours, and relative humidity are the results of point measurements. To be able to estimate the overall average of each set of the data over the catchment and over the lake, the Thiessen polygon approach was used. The Thiessen polygons were derived in Arc GIS using the DEM and position of the available synoptic weather stations (Figure 3-1). Then each polygon's area that overlapped the drainage basin, a_i and its relative area, a_i/A, were calculated, whereby the areal estimation of the each dataset was calculated both over the catchment and over the lake itself separately using equation (2-1) and (2-2) (Chow et al 1988).

$$\overline{P} = \frac{1}{A}\sum a_i P_i \qquad (2\text{-}1)$$

here, $\overline{P}$ is the areal estimation of the data quantity, P_i is data quantity for each station, a_i is the Thiessen polygon area for each station inside of the catchment or over the lake (Table 2-1) and A is the drainage basin area or the lake area, which is calculated as:

$$A = \sum a_i \qquad (2\text{-}2)$$

As indicated, in figure 2-2, in this method, the data of the stations even outside of the catchment can be used for areal estimation of the data over the catchment. In most of the previous studies on the Lake Urmia, only the data of Urmia station, station no. 15, which covers only 16% of the catchment area and 51% of the Lake area, has been used. But in this study, for a better estimation of all water balance components, most of the available data over the catchment and over the lake was used.

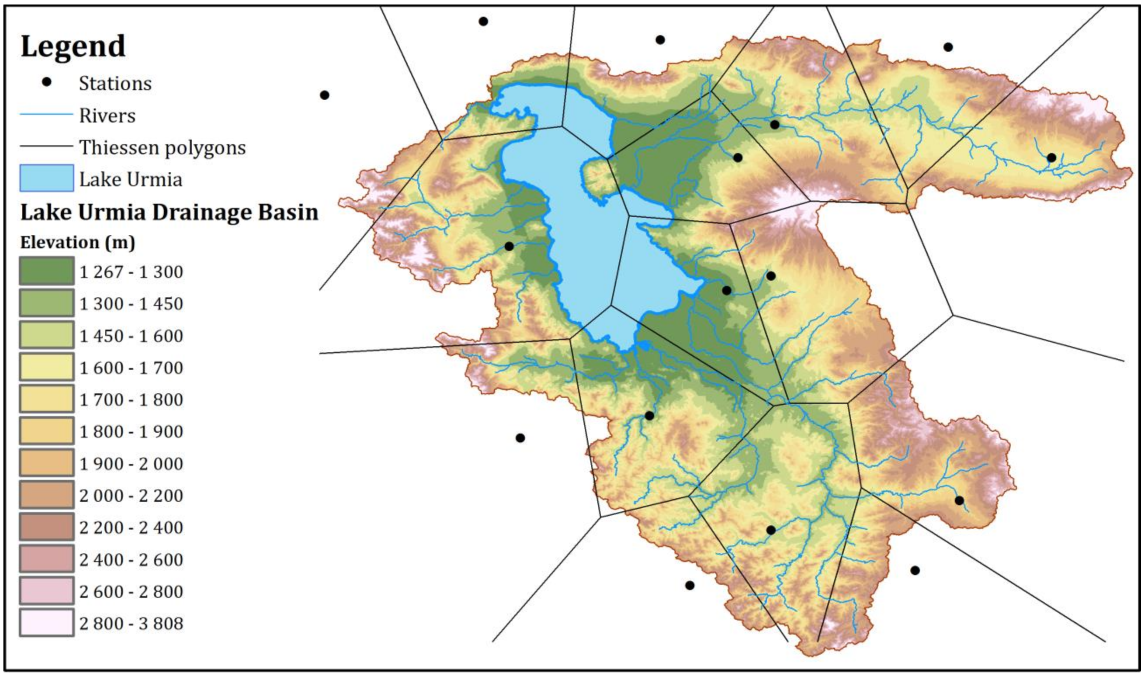

Figure 2-2. Lake Urmia catchment and synoptic weather stations with their Thiessen polygons

Table 2-1. Thiessen polygon multiplier for areal estimation of the data for both the basin and the Lake

no	Station	Basin	Lake	no	Station	Basin	Lake
1	Ahar	0,05	-	9	Sahand	0,06	0,04
2	Baneh	0,02	-	10	Salmas	0,01	-
3	Bonab	0,08	0,21	11	Saqqez	0,10	-
4	khoy	0,03	0,09	12	Sarab	0,07	-
5	Mahabad	0,10	0,06	13	Tabriz	0,08	-
6	Maragheh	0,08	-	14	Takab	0,07	-
7	Marand	0,04	0,09	15	Urmia	0,16	0,51
8	Piranshahr	0,02	-	16	Zarineh obatu	0,03	-

Since most of the data of the available stations was not complete, it was needed to estimate the missing data. Thus, first the monthly average of existing data of all stations was calculated as reference data using the Thiessen method, and then the monthly missing data was estimated based on the correlation between existing data of each station with the reference data. To do so, a linear regression was derived for each station for each set of data. But some of the stations were recently established with about only five years (60 months) of available data. Thus, for better areal estimation of the data the missing data was extrapolated for not measured years on a monthly basis. The average correlation coefficients (r^2) for precipitation, temperature, relative humidity and sunshine hours were 0.71, 0.99, 0.90 and 0.96 (See appendix C).

The measurement period of monthly data on sunshine hour was not as long as other data, but there was a strong positive correlation between temperature and sunshine hours (r^2 = 0.83 in average), therefore, not measured sunshine hour’s data was extrapolated using linear regression between monthly sunshine hours and monthly temperature for each station.

The lake’s monthly water surface temperature (WST) that was derived by Sina et al. (2013) estimated the Lake surface temperature only for eight month of the year without winter time for the years 2007-2010, thus, the four other months were estimated based on their correlation with monthly average atmosphere’s temperature over the lake at the same period of time using linear regression (r^2 = 0.99). Later on, a time series of the WST were generated from derived linear relation for the whole study period, to take account for the monthly and annual fluctuations.

Since most of the provided data was not complete, it was essential to complete the data for the favorable time period. Linear regression between each station and areal average of all station was used to estimate the missing data. In most of the cases there was a convenient relation between station data and the areal average data. But in some cases, because of smaller number of existing data, the correlation was not as strong as for the other stations.

2.3. Water balance of the Lake Urmia

To perform the annual water balance of the LUDB, the following equation was used (see section A.1):

$$\Delta S = P_{basin} - ETa_{basin} + P_{lake} - E_{lake} \quad (2\text{-}3)$$

where ΔS, is the change in the storage volume over a year $[L^3T^{-1}]$, ETa_{basin} is the total actual evapotranspiration from the drainage basin over a year $[L^3T^{-1}]$ and E_{lake} is the total annual evaporation from the water bodies in the basin $[L^3T^{-1}]$ and P_{basin} and P_{lake} are the total annual precipitation over the drainage basin and the lake $[L^3T^{-1}]$ respectively.

Thus, a MATLAB code was developed to calculate the Lake's water level for each year based on the water level of the previous year and a calculated change in the lake volume (ΔS) assuming that the lake area (and level) over the course of a year adjusts such that the net water loss from the lake (P_{lake}-E_{lake}, where $E_{lake}>P_{lake}$) equals the net water gain from the basin (P_{basin}-ET_{basin}, where $P_{basin}>ET_{basin}$). To start the simulation the Lake Urmia's water level at the beginning of the simulation period was needed as an input data. The necessary input data to calculate all components of the equation 2-3 was the annual precipitation, annual temperature both over the lake and the drainage basin and sunshine hours, relative humidity and atmosphere pressure over the lake. The model then calculates the ETa_{basin} and E_{lake} by means of input data to solve the water balance equation.

2.3.1. Evaporation

To calculate the evaporation from the lake, the energy balance approach was used and then pan evaporation measurements were used as an independent source to validate the model's results.

Energy balance approach

Evaporation from a water body can be calculated using energy balance method as:

$$E = \frac{K + L}{\rho_w \cdot \lambda v \cdot (1 + B)} \quad (2\text{-}4)$$

where E is evaporation, K is shortwave radiation, L is longwave radiation, ρ_w is water mass density and λ_v, is the latent heat of vaporization and B is Bowen ratio. The detailed method of calculation of each component of equation 2-4 is given in appendix A (section A.3.2).

A MATLAB function was developed to estimate the monthly and annual evaporation based on the lake latitude, monthly atmosphere temperature over the lake, monthly water surface temperature of the lake, atmosphere pressure, sunshine hours and relative humidity.

In the calculation procedure, in equations (A-18) and (A-21), cloudiness is needed. But since there was not any measured data available for cloudiness, sunshine hour's data was used to estimate it. Thus the duration of each single day of each month was calculated using equation (A-4) and was summed up for each month to calculate the total monthly day duration and thereby calculate the cloudiness as:

$$C = 1 - \frac{monthly\ sunny\ hours}{total\ day\ durations\ of\ each\ month\ (hrs)} \qquad (2\text{-}5)$$

where C is cloudiness.

To estimate the albedo of water surface, equation A-19 was used. But since in this empirical model, the albedo is a function of incoming solar radiation (K_{in}) which itself is a function of albedo (equations B-6 and A-18), thus an iteration method was used to estimate the albedo with the precision of 1%. Hence instead of constant albedo for water surface, it varies during the year.

The method outlined in the section A.3.2 estimates evaporation from fresh water, but, since the salinity of the Lake Urmia's water was extremely high, which put it in "brine" class based on classifications, its saturation vapor pressure is less than the fresh water saturation vapor pressure. Thus to estimate the saturation vapor pressure of the brine, equation 2-6 was used (Salhotra et al, 1985):

$$e^{*}_{Braine} = \beta \cdot e^{*}_{fresh\ water} \qquad (2\text{-}6)$$

Where, β is the activity coefficient of the water defined as "the ratio of vapor pressure of saline water to vapor pressure of fresh water at the same temperature". The value of β is a function of the salinity of the evaporating water (Figure 2-1). In the Lake Urmia, Sodium Chloride (NaCl) is the main substance of the salinity of the lake water with approximately 90% of total dissolved solids (Table 1-2). Thus only the effect of the NaCl in the figure 2-2 was considered on the calculation of the water activity coefficient (β).

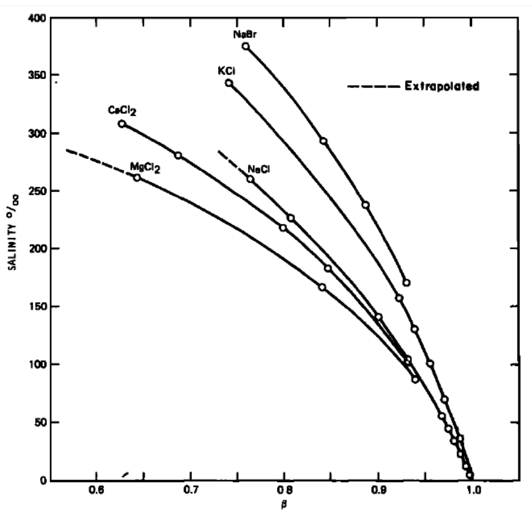

Figure 2-2. Activity coefficient of water as a function of salinity at 20°C for solutions of different ionic composition ((Salhotra A. M. et al, 1985)

Moreover, the density of water also changes with its salinity. Therefore, the density of the Lake Urmia's water was calculated as:

$$\rho_s = \rho_0 + A \cdot S + B \cdot S^{3/2} + C \cdot S^2 \tag{2-7}$$

where, ρ_s, is the density of saline water, ρ_0 is the density of pure water, S is salinity in (‰), C is constant (C = 4.8314×10^{-4}), A and B are functions of temperature which is defined as (McCutcheon, et al 1993):

$$\begin{aligned} A = {} & 8.24493\times10^{-1} - 4.0899\times10^{-3}\cdot T \\ & + 7.6438\times10^{-5}\cdot T^2 - 8.2467\times10^{-7}\cdot T^3 \\ & + 5.3675\times10^{-9}\cdot T^4 \end{aligned} \tag{2-8}$$

$$\begin{aligned} B = {} & -5.724\times10^{-3} + 1.0227\times10^{-4}\cdot T \\ & -1.6546\times10^{-6}\cdot T^2 \end{aligned} \tag{2-9}$$

The salinity data of the lake was derived from previous studies (Abbaspour & Nazaridoust 2007). Then the relation between Lake water level and its salinity was derived using linear regression. To prevent the estimation of salinities over the solubility of NaCl in extremely low water level, maximum solubility of NaCl was introduced to the model for different temperature (Table 2-3) using a quadratic equation.

Table 2-3. Maximum solubility of the NaCl in different temperature (Wikipedia 2014)

Temperature (°C)	Solubility (g/l)
0	356.5
10	357.2
20	358.9
30	360.9
40	363.7

Pan Evaporation

The evaporation from a saline water body can be calculated as:

$$E = \Theta \cdot k_p \cdot Ep \tag{2-10}$$

where, Ep is the evaporation from the pan, k_p is the pan coefficient which is (0.7-0.8) for the Class-A pan (Chow et al. 1988) and Θ ($0 \leq \Theta \leq 1$) is a ratio of evaporation of saline water to the evaporation of freshwater.

In this work the pan evaporation of closest station to the lake (i.e. Golmankhaneh station) was used. In the mentioned station, evaporation of both fresh and saline water was measured using class-A pans. But the duration of measurements was limited (1989-2005), while average fresh water pan evaporation of the LUDB was available for longer periods. Thus the fresh water pan evaporation of the Golmankhaneh station was extrapolated using linear regression (r^2 =0.99) based on the average fresh water pan evaporation of the LUDB. Then Θ was calculated by means of the relation between fresh and saline water pan evaporation measurements in the Golmankhaneh station (r^2 = 0.99). To account for the effect of dramatic change in the salinity of the lake on Θ, the correlation between salinity of the lake and saline water pan evaporation was derived using linear regression, and the updated Θ was used in calculations (see appendix C). Base on the regional water authority report, suitable pan coefficient for the used class-A pans in the LUDB is suggested to be $k_p = 0.77$ (Mohammadi 2005).

2.3.2. Evapotranspiration

The evapotranspiration in the LUDB was estimated using Turc-Langbein method:

$$ETp = 325 + 21T + 0.9T^2 \tag{2-11}$$

$$ETa_{basin} = \frac{P_{basin}}{\sqrt{0.9 + \frac{P_{basin}^2}{ETp^2}}} \tag{2-12}$$

where, ETp is the annual potential evapotranspiration (mm) and T is the average annual temperature over the land (°C) and ETa_{basin} is the actual annual evapotranspiration (mm).

In order to check the validity of actual evapotranspiration calculated from this method other independent estimation of Eta was needed. Hence the monthly evapotranspiration raster data with 8km resolution of Moderate Resolution Imaging Spectroradiometer (MODIS) provided by NTSG (2014) was used. The boundaries of the LUDB were roughly estimated by a rectangular to mask the monthly raster and calculate the overall average of the monthly evapotranspiration over the catchment (Figure 2-4). The cells over the lake were also roughly estimated and removed to avoid the confusion between evaporation over the lake and evapotranspiration over the terrain.

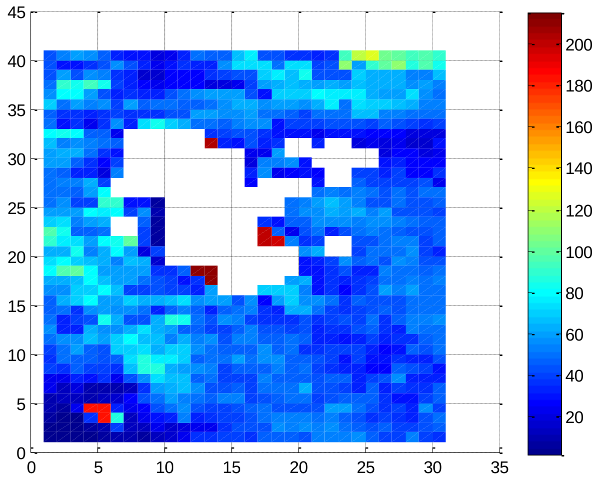

Figure 2-4. Monthly evapotranspiration over the Lake Urmia basin from MODIS for the June 2004

2.3.4 Irrigation

To estimate the irrigation in the LUDB, first the total irrigated area located in the basin was estimated, then assuming an area-normalized Irrigation Requirement (IR), the total annual water volume used for irrigation was estimated. The data of the total irrigated land area was available only for the year 2012 (ULRP 2014). However Nasiri (2003) studied the land use change in the ecological zone of the Lake Urmia for the period of 1990 till 2000. It is also mentioned at the ULRP's website, that the irrigated area has increased from 300000 (ha) to 500000 (ha) in the past three decades.

To estimate the irrigated land area in the study period, the rate of the development in the whole basin was assumed to be the same as the mentioned values in ULRP' website , whereby a linear relation was derived to estimate the irrigated land in each year for the study period. This estimation however, does not account for annual fluctuations around the mean trend of the irrigated agricultural land according to water availability constraint for each year.

The assumed irrigated area based on the data point of 2012 and assumed development rate of the period of 1979- 2012 is given in figure 2-5. Thus the irrigated area of 226555 (ha) at year 1965 increases to 499282 (ha) at year 2010 by the constant increase rate of 6061 hectares per year.

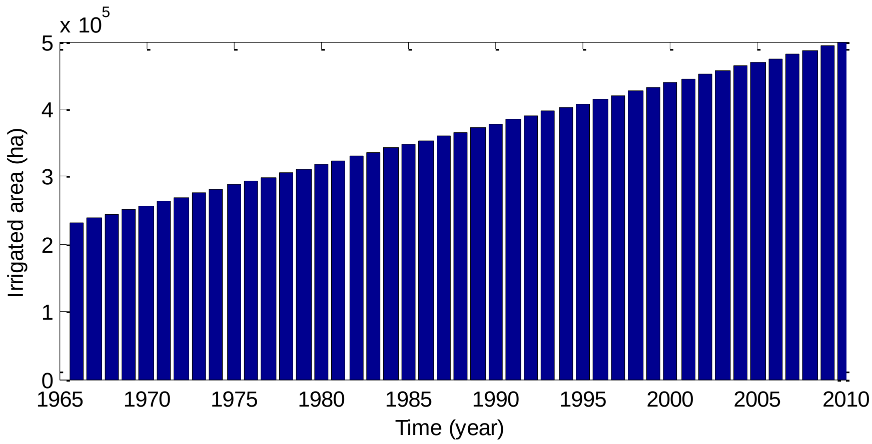

Figure 2-5. Assumed increase in irrigated area over the whole LUDB

The IR is the daily maximum water volume needed to be supplied through the irrigation system to fulfill the Crop Water Requirement (CWR), which depend on the crop type and climatic conditions (Savva and Frenken 2002). In this study IR was assumed to be 1(lit/s/ha) for a seven months period, which in fact equals the water allocation quantity, issued by local authorities (West Azerbaijan regional water authority and Kurdistan regional water authority).

Assuming 1lit/s/ha for IR, the total irrigation water requirement increases from4.11km^3 at 1965 to 9.06 km^3 at 2010. In this assumed irrigated agricultural area, any fluctuation due to availability of water is ignored. In other words, farmers use as much land as possible with the available water. Thus in draughts, for instance, they cannot supply water for all previous irrigated lands which results in the decrease in irrigated land area or prevent further development. This means using linear interpolation of irrigated agricultural land development, may over-estimate the irrigation in draughts. This flexibility however, is possible only in annual plants farms. Thus changing the cropping pattern from annual plants farms to orchard may lead to over use scarce water in draughts. Thus developing orchard based on wet years may lead to over use of water resources in normal years.

To introduce irrigation to the model, the irrigation water was subtracted from the calculated surplus runoff (*R*=*P*-*ET*) and was added to the precipitation as an additional precipitation (Törnqvist and Jarsjö 2012). The ET due to irrigation was then calculated by subtracting the natural ET from the ET resulting from the modified P (with added irrigation). Finally the total runoff (R_{total}) was estimated by subtracting the ET due to irrigation (ETa_{ir}) from the natural R (see equations 2-13 till 2-15 and figure 2-6).

$$P_{new} = P + irrigation \tag{2-13}$$

$$ETa_{ir} = ETa_{new} - Eta \tag{2-14}$$

$$R_{total} = R - Eta_{ir} \tag{2-15}$$

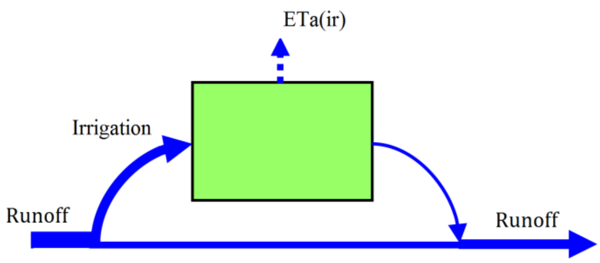

Figure 2-6. Introducing irrigation to the model (Törnqvist and Jarsjö 2012)

2.4. Calibration of the model

The only calibration performed in the model was the calibration of ET. The ET calculated from Turc-Langbein method, caused the collapse of the lake even without irrigation. Thus, the first five years of the simulation (1965-1969) – with lowest irrigation – was used to calibrate ET. The ET calibrated such that to reproduce the observed lake water level during the calibration period. Then to control the accuracy of the calculated ET, the results were compared with the ET data of MODIS. The final ET used in the model was set to 84% of the results of the Turc-Langbein method.

2.5 Validation of the model

As mentioned before, the first five years of the data (1965-69) was used for calibration of the model. The rest of the available historical data (1970-2010) was used to check the validity of the model. To assess the results of the model, Root Mean Square Error (RMSE) of estimated WL was calculated (Equation 2-16).

$$RMSE = \sqrt{\frac{(WL_O - WL_E)^2}{n}} \quad (2\text{-}16)$$

where WL_O and WL_E are observed and estimated water level respectively.

2.6 sensitivity analysis

Since the model was calibrated with regard to ET and since the value of IR is uncertain, a sensitivity analysis of the model was assessed considering these two variables. The change in the final water level at the end of the study period (2010) relative to its original calibrated value was assessed against the applied change in each variable during the whole period. In the case of ET, the coefficient used to calibrate the model, which represents the percentage of the results of Turc-Langbein method, was varied between 75% and 90%. To evaluate the effect of IR on the final water level estimations, the IR values were varied between very low, 0.5 lit/s/ha and very high 3 lit/s/ha. The water level at the end of the period was calculated for each IR.

2.7 Main causes of the lake's shrinkage

LUDB has been subjected to ambient changes that in recent years led to dramatic decrease in the lake's water level and thus its area and volume. As mentioned before, there has been an aggressive irrigated agricultural land development in the basin. Three main variable i.e. annual precipitation, mean annual temperature and agricultural land area, were studied for their effect on the lake's water level. Thus different scenarios were defined to simulate the change in the selected variables.

The scenarios were designed to study the effect of the change in the three main variables on the lake's water level. Hence beside the original scenario in which everything was assumed as the historical data, three more scenarios were defined. At the first scenario, the precipitation of the period of 1996-2010 is increased, in the second scenario the temperature of the period of 1996-2010 is decreased and in the final scenario it was assumed that no agricultural development had happened in the LUDB and the irrigated land remained the same as 226554.5 ha in the year 1965. Furthermore, a scenario (P4) was defined to represent the effect of recent agricultural development, after 1995, in which from the year 1996 the agricultural land area remained the same as the year 1995 (table 2-6).

Table 2-4. Change in the main selected variables in defined scenarios.

Scenario	Agriculture (ha) (1965-2010)	Precipitation (mm) (1996-2010)	Temperature (℃) (1996-2010)
P0	-	-	-
P1	226555	-	-
P2	-	+78	-
P3	-	-	-0.7

2.8 Future projections

There are different possible future pathways for the lake water levels depending on the future pathways of climate change and land use change in the LUDB. Different scenarios were defined to simulate the future of the lake WL. Several simulations were performed based on various predefined scenarios of the future conditions. Climate change alternatives were: no-change, best case change and worst case change. Land use change alternatives were: no-change and change at the same rate as shown by historical data.

The climate change data was derived from Intergovernmental Panel on Climate Change's (IPCC) report. The IPCC report on climate change is based on multi-model mean results, which makes it more reliable. The climate change in the IPCC report is presented as the projected change of climate components of the period of 2081-2100 relative to 1986-2005 for different scenarios (IPCC 2013). The future climate change components were introduced to the model as a linear change between the midpoints of the two periods i.e. 1996 to 2091. Four different future pathways are reported based on Representative Concentration Pathways (RCP) to simulate the future climate (Detlef P. et al 2011). In this study future climate projections based on two scenarios RCP2.6 and RCP8.5 were used as the best and the worst case scenarios respectively (Figue 2-7). The results of Coupled Model Intercomparison Project Phase 5 (CMIP5) for temperature and precipitation for 2081-2100 are given in figure (2-6). Based on the changes shown for the considered region in this figures the change in temperature was assumed to be 1.5°C and 7°C and change in precipitation was assumed to be 0% and -15% for RCP2.6 and RCP8.5 respectively .

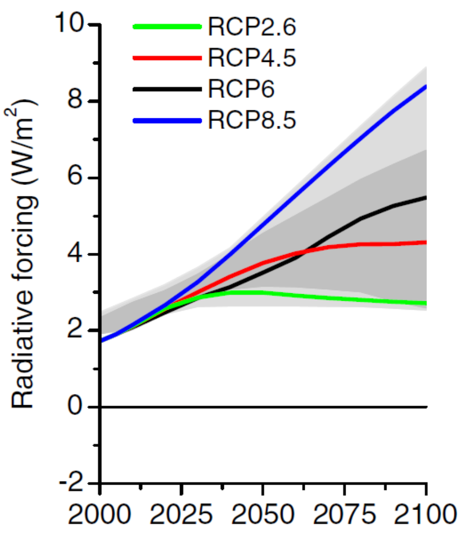

Figure 2-7. Four representative concentration pathways (RCP)

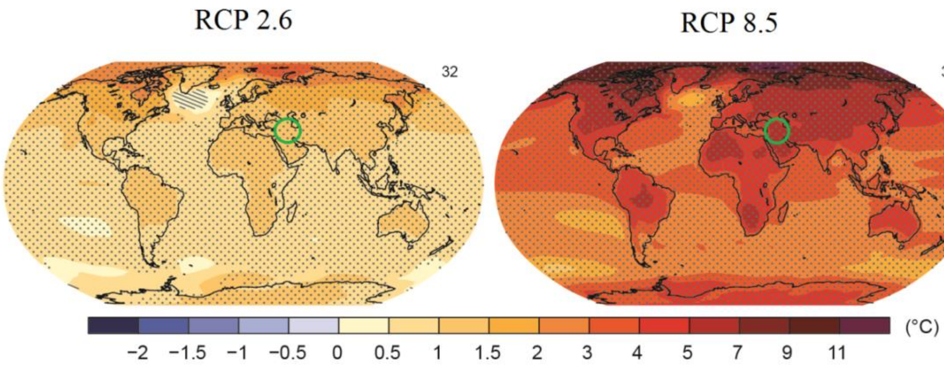

(a)

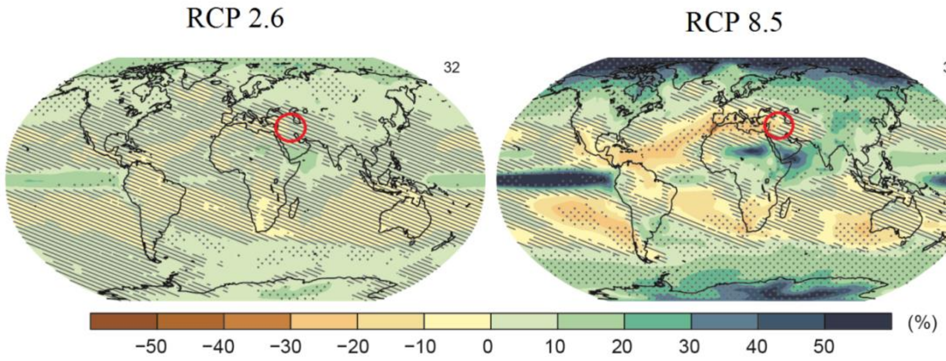

(b)

Figure 2-8. Results of CMIP5 multi-model for the scenarios RCP2.6 and RCP8.5 in 2081–2100 of (a) annual mean surface temperature change and (b) average percent change in annual mean precipitation relative to 1986-2005. The number at the upper side of the maps indicate the number of models used in projections (i.e. 23 models for RCP2.6 and 39 models for RCP8.5)

2.8.1 Future scenarios

Future scenarios were defined by assuming different combinations of future values of the input variables i.e. annual irrigated land area, precipitation, temperature, relative humidity and sunny hours. The amount of the irrigated land at the beginning of the simulation was derived from the linear relation presented in section 2-3-4. For the climatic variables (i.e. precipitation, temperature, relative humidity and sunshine hours), the data derived from the IPCC report was used. To do so, for each set of the data the average of the historical observed values for the period of 1986-2005 (the same period used in the CMIP5 multi-model) was calculated. Then the average of climate components (i.e. precipitation and temperature) for the period of 2081-2100 were calculated using projected changes derived from results of CMIP5 multi-model (figure 2-8) and the average of the period of 1986-2005. A linear relation was derived between the mid-points of the two periods to interpolate the data during the simulation period. Since the simulation period started from 2012, the values of the starting point were interpolated from the derived linear relation. The relative humidity and sunshine hours were assumed to be constant during the simulation period and equal to the average of the base period (1986-2005).

Using combination of future projections for climate change and agricultural land use change, different scenarios were defined. All defined scenarios are presented in table (2-5).

Table. 2-5. Defined scenarios based on climate change and irrigated land use change.

Scenario	Irrigated land change	Climate pathway
0	no change	no change
1	no change	RCP2.6
2	no change	RCP8.5
3	change	no change
4	change	RCP2.6
5	change	RCP8.5

3. Results

3.1. Historical trends of precipitation and temperature

There is a significant decrease (in 95% level – t-test) in the annual precipitation after the year 1995 by 78 mm relative to the period of 1965-1995 (Figure 3-1). There is also a significant increase (in 95% level – t-test) in the average annual temperature for the same period by 0.7℃ relative to the period of 1965-1995(Figure 3-2).

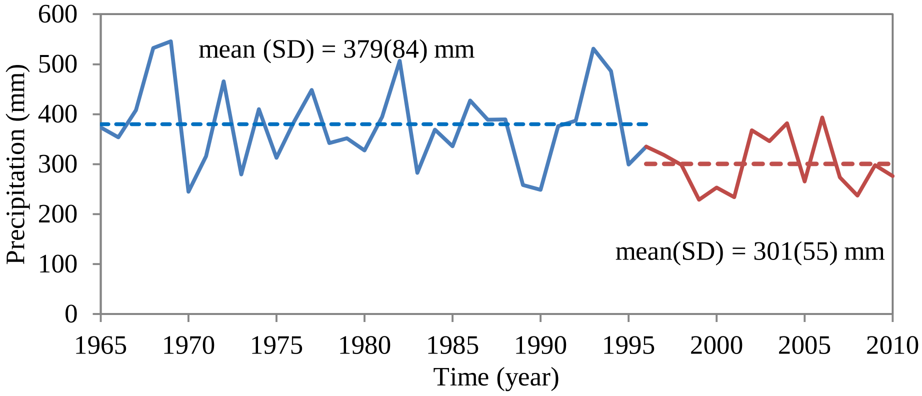

Figure 3-1. Change in annual precipitation in LUDB

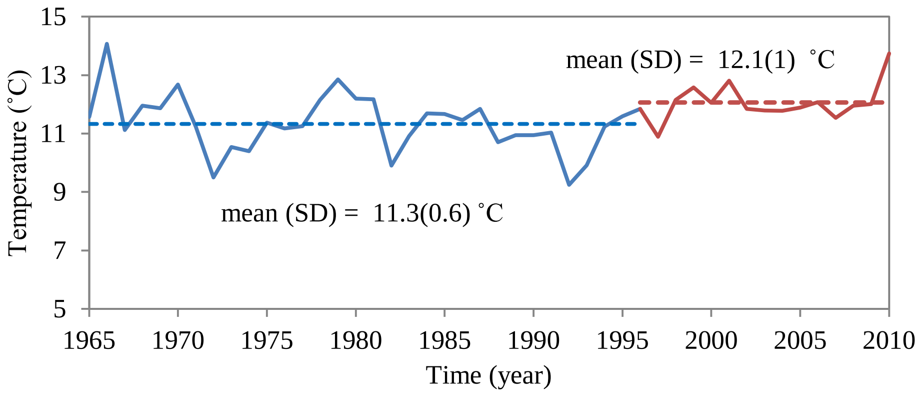

Figure 3-2. Change in annual temperature in LUDB

3.2. Water balance

3.2.1. Evaporation

The results of the energy balance estimation and pan measurement of monthly average evaporation over Lake Urmia is given in figure 3-3. Although the match is generally good, in the majority of the summer months with high evaporation, the energy balance method gives higher values than those derived from pan evaporation. But in the colder months the evaporation from energy balance method is smaller than the pan evaporation. The highest evaporation occurs in summer time, June, July and August and the lowest evaporation belongs to winter times.

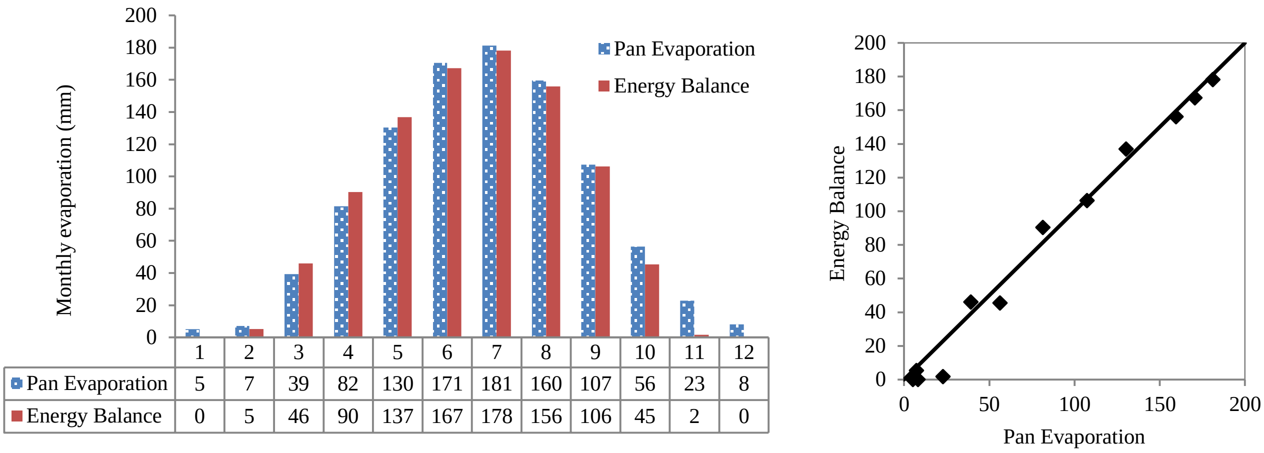

	1	2	3	4	5	6	7	8	9	10	11	12
Pan Evaporation	5	7	39	82	130	171	181	160	107	56	23	8
Energy Balance	0	5	46	90	137	167	178	156	106	45	2	0

Figure 3-3. Average monthly evaporation over the Lake Urmia (mm)

The estimated annual evaporation which equals the sum of estimated monthly evaporation for each year is shown in figure 3-4. Since the estimated monthly evaporation is consistent with the measured data, the annual estimated evaporation is also in a relatively good match with observed data. The RMSE of the annual estimation is 102 mm which is 10% of the observed average annual evaporation estimated using fresh water pans. The annual average of evaporation estimated using the energy balance method was 932 mm while the corresponding estimate based on pan evaporation measurements was 972 mm.

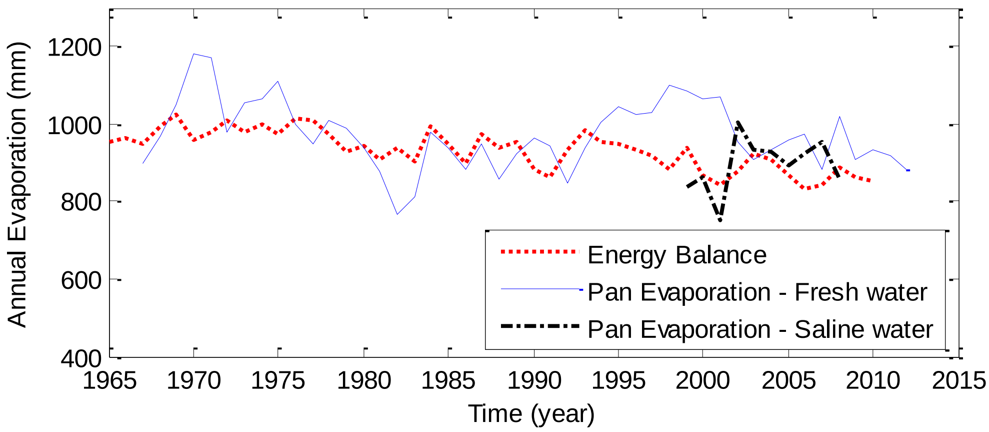

Figure 3-4. Annual evaporation over the Lake Urmia (mm)

3.2.2. Evapotranspiration

Actual evapotranspiration (ETa) is one of the main components of the model and as mentioned before, it was a main calibration variable in the model. Since there was no direct measurement of the evapotranspiration in the Lake Urmia drainage basin, to validate the results of the Turc-Langbein approach, remote sensing data of MODIS was used. Results of ETa calculated by Turc-Langbein method after calibration (including evapotranspiration due to irrigation) and from the data of MODIS are given in figure 3-

5. The annual average evapotranspiration were estimated as 287 and 270 (mm/yr) from Turc-Langbein and MODIS data respectively. As indicated, comparing with MODIS data, the evapotranspiration from Turc-Langbein method is slightly higher than the MODIS data and have higher fluctuations. However, Figure 3-5 shows that the evapotranspiration results overall are relatively similar. Since the calibration of ETa was independent of MODIS data, the consistency of the results of the two methods may interpreted as the validity of the results of Turc-Langbein method used in the water balance model.

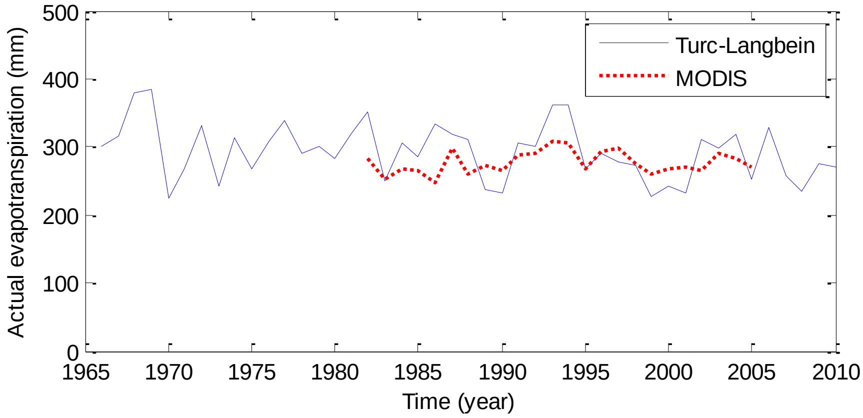

Figure 3-5. Estimated annual evapotranspiration of the Lake Urmia basin for the period (1965-2005)

3.2.3. Lake water level

Figure 3-7 indicates the simulated and observed water level of the Lake Urmia with the calibrated evapotranspiration for the first five year (1965-1969). The maximum error of simulation is 1.03 (m) that is 6.4% of the maximum depth of 16 (m) and 17% of average depth. RMSE of simulation is 0.40 (m) i.e. 2.5% of maximum depth and 6.7% of average depth. Figure 3-6 indicate that there is a good match between estimated and observed water level. However as indicated in figure 3-8 the error of simulation is not completely random and has a periodic pattern which can be approximated by a sinusoidal function. In other words, the model either over estimate or underestimate the lake's level periodically.

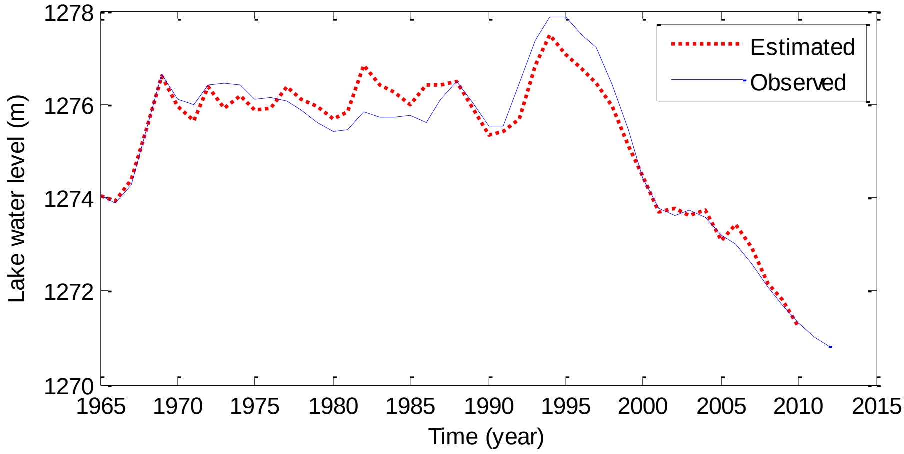

Figure 3-6. Water Level of the Lake Urmia without any additional calibration (RMSE = 396 mm)

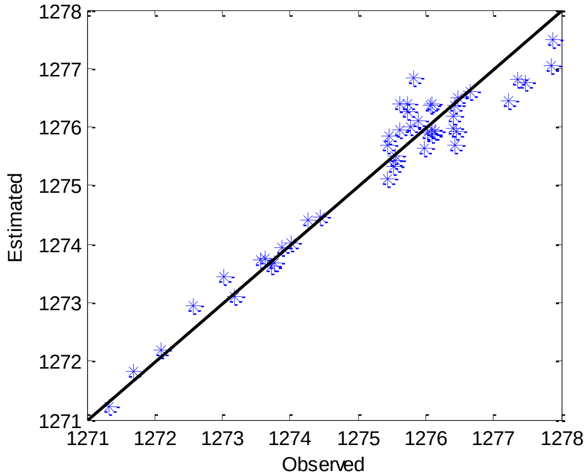

Figure 3-7. Estimated water level versus observed water level of Lake Urmia

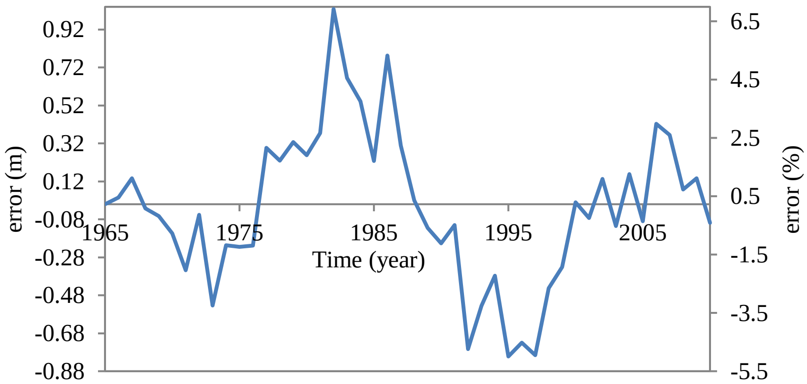

Figure 3-8. Error of simulation of the Water Level of the Lake Urmia

3.3. Sensitivity analysis

In the case of calibration or subjective decision on variables in modeling, sensitivity analysis indicate, how uncertainty in inputs may affect the uncertainty in the results. Figure 3-9a indicates the change in the water level at the end of the period relative to calibrated model results, as a result of change in evapotranspiration coefficient, and figure 3-9b shows the change in the water level at the end of the period against different values of IR.

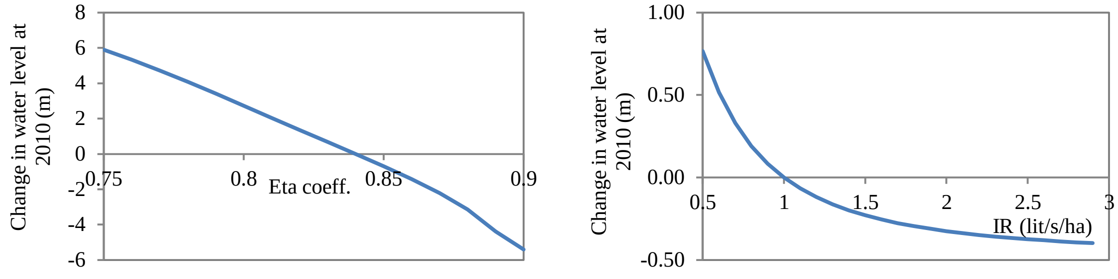

Figure 3-9. Change in the water level at the end of study period (2010) as a result of change in a) evapotranspiration coefficient (Eta-coeff.) b) irrigation requirement (IR)

As indicated in the figure 3-9, the results of the model are highly sensitive to the Evapotranspiration coefficient and in average, by 0.01 unit change in the coefficient, the water level at the end of the period, changes by 0.75 m. In the other hand, the model is less sensitive to the IR. However the model is more sensitive to the lower value of IR relative to its higher values which in fact is more likely.

3.4. Main drivers of the lake's thus for observed shrinkage

Results of simulations based on the defined past scenarios (Table 3-6), is presented in figure 3-10.

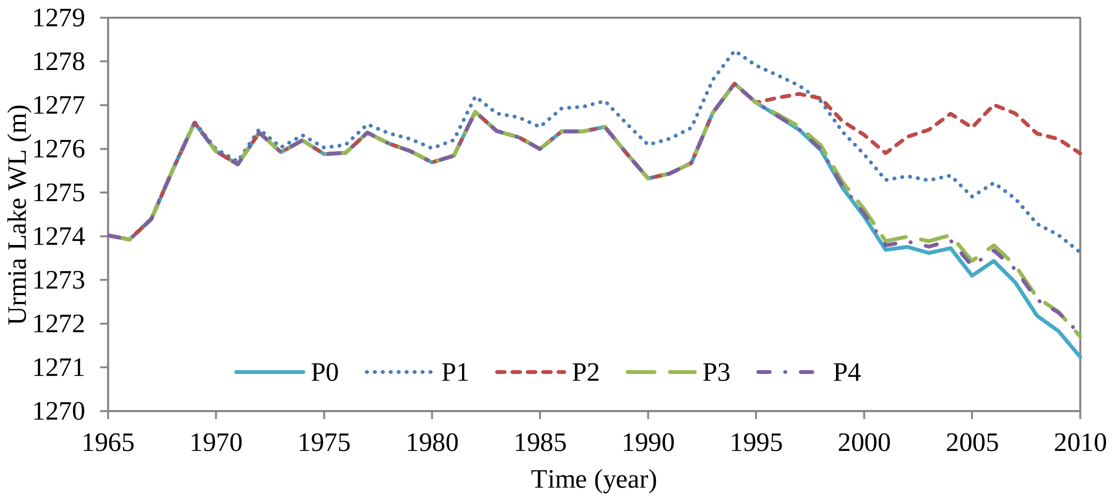

Figure 3-10. Water level of the Lake Urmia based on the four defined past scenarios (Table 3-6) i.e. no irrigated agricultural area development in the basin (P1), no decrease in precipitation after the year 1995 (P2), no increase in temperature after the year 1995 (P3) and no agricultural development after the year 1995 (P4)

As indicated in Figure 3-10, if one removes the observed average decrease in precipitation of 78 mm/year during the last 15 years of the study period (1996-2010), the effect is large on the lake's water level with 4.66 m increase in the water level at the end of the period (2010). Second most important variable that affected the lake's water level is the irrigated agricultural development in the basin from the beginning of the study period (1965). It changed the water level of the lake at the end of the period by 2.40 m. Recent agricultural development and temperature decrease however, showed minor effects on the lakes water level with only 0.5 m change in the water level in the year 2010. Thus based on these simulations, 62% of the recent decrease in the Lake Urmia's water level is due to decrease in precipitation after the year 1995 (Figure 3-11), whereas water development plans is responsible for 32% of the negative water balance in the LUDB.

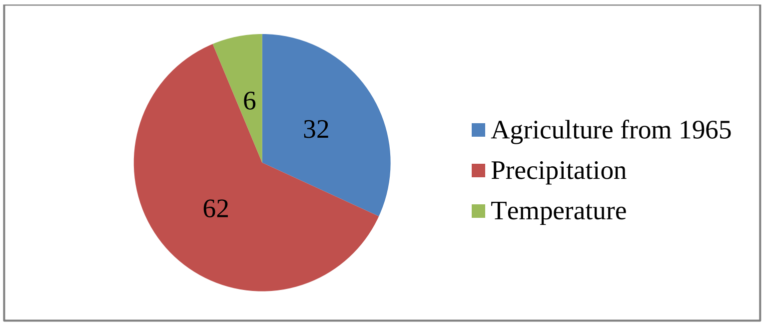

Figure 3-11. Main factors affecting the Lake Urmia's water level

Previous studies (Hassanzade et al. 2012) have concluded that the decrease in inflow to the Lake Urmia is the main factor with 65% effect. Since the change in inflow can be the effect of both climate and human induced changes in the basin, and considering that precipitation over the lake itself contributes by 10% to the shrinkage according to their assessments, while the drainage basin is approximately ten times bigger than the lake, their results can be viewed as consistent with the results of current study on the large effect of precipitation.

3.5. Future projections

The results of the simulations between 2012 and 2050 are given in figure 3-10 and table 3-2. The dashed lines in the figure indicate the scenarios with no change in irrigation for three different climate change scenarios (S0, S1 and S2) while the solid lines represent the scenarios with change in irrigation for different climate change conditions (S3, S4 and S5). The asterisk point represents the current observed position (2015) of the Lake Urmia water level. The ecological WL (Eco) and the lowest water level in dried lake (Zero) based on the Lake Urmia's bathymetry relations are also shown in figure 3-10. The observed water level is also shown before 2012.

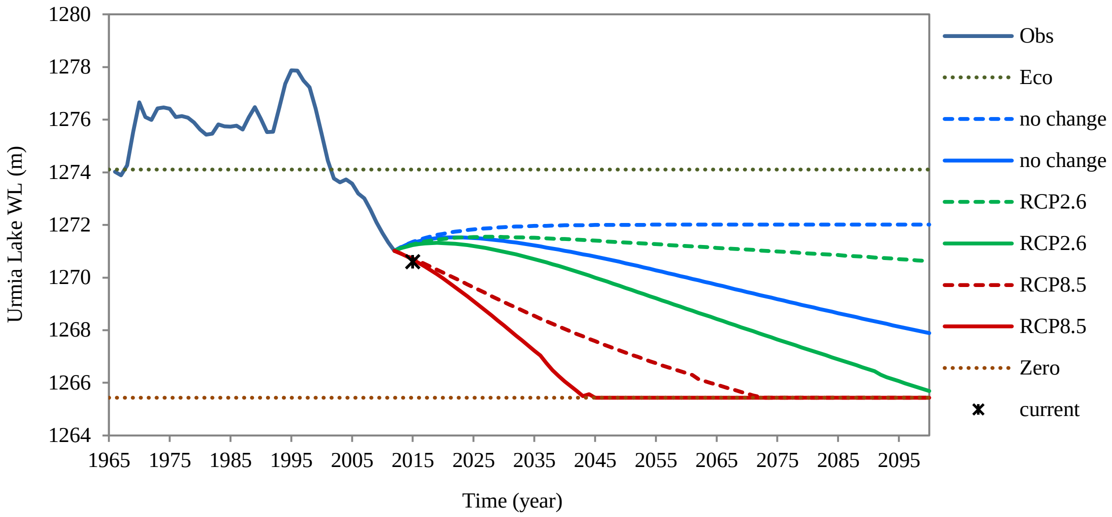

Figure 3-10. Future projection of the Lake Urmia water level for different climate scenarios and with (solid lines) and without (dashed lines) irrigated agricultural land development

Since the simulation started from 2012, the current position (2015) can be a checking point for the future projections. As indicated in figure 3-10 and table 3-1, none of the scenarios except for the worst case scenario of the climate pathways (RCP8.5) is close to current level of the lake. Except for the RCP8.5 scenarios, all other scenarios show an improvement in the lakes condition in at least the near future (2020) but none of them will reach the ecological water level (1274.1 m) of the lake. Two of climate pathway scenarios (no change and RCP2.6) predict the higher water level for the lake at the year 2015 relative to the current water level of (1270.59 m). This could be a result of higher precipitation and lower temperature at the starting point (2012) relative to corresponding observed values. While the difference between different climate scenarios is large, the effect of agricultural land use change is smaller yet considerable. Scenarios with RCP8.5 climate pathway have the worst effect on the lake's condition and its results are closer to the observed water level at 2015. This could means that either the worst case scenario of both climate change and agricultural land use change is happening, or it is the effect of periodic droughts along with milder climate change and agricultural land use change. Based on the simulations results, there is no hope for the recovery of the lake and in the best case scenario, it will not dry up any more but the WL never reaches the ecological WL. In the worst case scenario the lake will dry up completely before 2045.

Considering the uncertainty in the lower depths (bathymetry relations are extrapolated for depths under 1271 (m)) the shrinkage of the lake may differ from what is presented.

Table 3-1. Future projection of the Lake Urmia water level for the years 2015, 2020, 2050 and 2100

			2015		2020		2050		2100	
Scenario	Change in irrigation area	Climate change	WL	Change relative to 2012 (m)	WL	Change relative to 2012 (m)	WL	Change relative to 2012 (m)	WL	Change relative to 2012 (m)
S0	no change	no change	1271.35	0.33	1271.67	0.65	1272.00	0.98	1272.01	0.99
S1	no change	RCP2.6	1271.26	0.24	1271.47	0.45	1271.33	0.31	1270.62	-0.4
S2	no change	RCP8.5	1270.73	-0.3	1270.19	-0.8	1267.15	-3.9	1265.43	-5.6
S3	change	no change	1271.32	0.3	1271.51	0.49	1270.54	-0.5	1267.89	-3.1
S4	change	RCP2.6	1271.23	0.21	1271.31	0.29	1269.61	-1.4	1265.68	-5.3
S5	change	RCP8.5	1270.68	-0.3	1269.97	-1.1	1265.43	-5.6	1265.43	-5.6

Considering the scenario S5 (since its results is closer to the current water level) the model predict on average 0.047 (m) increase in the Lake Urmia's water level at the year 2020 per each millimeter increase in the annual precipitation for the whole period (2012-2020) assuming no change in other variables. This increase is 0.059 (m) per 0.1˚C decrease in annual temperature and 0.007 (m) per each 1000 (ha) decrease in irrigated land area at the beginning of the period. These results imply that even with 20% decrease in irrigated agricultural area (100000 ha) with the current climate condition, the lake water level will recover only by 0.7 m in the year 2020.

According to the results of current study, given the observed annual 932 mm of evaporation from the lake and average annual precipitation of 269 mm over the lake during the past fifteen years with the average area of 5000 km^2, Lake Urmia needs at least 3.315 km3 inflows to compensate the excessive evaporation and stay steady. This value is 3.05 km3 given the long term annual average of precipitation i.e. 322 mm.

4. Discussion

Based on the current study, decreased annual precipitation since 1995 is identified as the main factor causing the changes in the Lake Urmia's water level and volume and agricultural development during the study period was the second most influential factor.

Since the water level is a function of the lake's volume, any approximation in the lake's volume can affect the water level estimation. Thus accuracy of the lake's depth-area-volume relation (estimated in a previous study) has a great effect on the model's results. Moreover, in this model, possible effects of multi-annual storage in the drainage basin were neglected; these may delay the response of the lake.

We here considered the agricultural water which account for 90% of the total water use. The population increase has led to increase in domestic and industrial water however, its effect on the lake's water balance is limited because the amount of water use is small relative to the agricultural use. Assuming all water in the closed basin either enter the atmosphere through evaporation and evapotranspiration or reach the lake as surplus runoff, the effect of storage increases due to water regulation plans in the basin is neglected. In other words, the effect of 2.0 km^3 regulating volume of the dams i.e. 12% of the Lake Urmia's volume at the ecological water level (1.7 km^3) is neglected. Even given the uncertainty in irrigated agricultural area, the model still simulates the water level of the lake with an acceptable estimation error especially in the range of levels the depth-area-volume measurements have been performed. Thus the model may be helpful for future projections and in assessing different restoration plan of the lake.

In comparison with the Lake Van, despite the similar behavior until 2002, the decrease in Lake Urmia's water level continues, while Lake Van is recovering until 2007. Figure 3-20 indicate the relation between annual water level changes relative to the previous year in the two lakes. On the other hand, since the Lake Van with the maximum depth of 451m is much deeper than Lake Urmia, water level changes of The Lake Van may have a smaller effect on the lake's, area and ecosystem. Furthermore, larger basin of Lake Urmia may increase the Lake Urmia's sensitivity to the any changes in the basin.

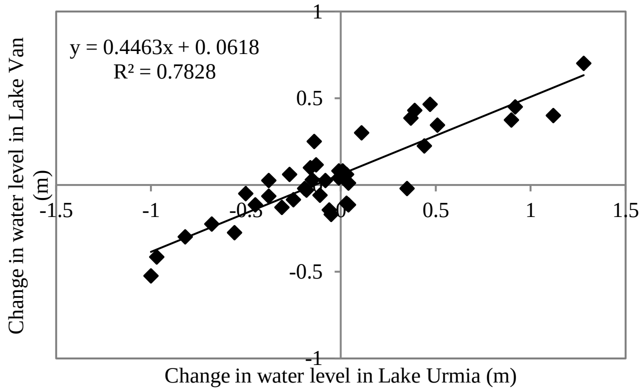

Figure 4-1. Relation between water level change in the Lake Urmia and in the Lake Van relative to previous year

Lake Urmia is not a unique lake facing a challenge of desiccation. There are several other lakes and wetlands worldwide facing the same challenge.

Aral Sea has lost more than 50% of its surface and two-third of its volume due to excessive water diversion from the two main input rivers. According to Destouni et al. (2010) 80% of the input runoff to the Aral Sea is diverted for irrigation that lost through evapotranspiration led to drastic shrinkage of the Lake. But despite the several extensive studies, the main process of changes is a matter of debate (Cretaux et al. 2013).

Beaverhills Lake a 140 km^2 shallow wetland, an international Ramsar site, located in central Alberta, Canada, dried up completely in 2006 which according to Dekker (2014) was the results of anthropogenic interference in the Lake's basin along with a cycle of drought. But based on long-term data of the region, there is no support for climate change as the main factor of dry up of Beaverhills Lake (Dekker 2014).

Chunlan et al. (2006) investigated the reasons of shrinkage of the Baiyangdian Lake wetland, the only large fresh-water lake in the Northern Chana plain, and blamed the warming temperature and decreased precipitation as the main ruling factors. Anthropogenic changes in the basin, however were not the main ruling factors, but accelerated the degradation due to climatic changes.

Owens Lake dried up as a result of water diversion by the city of Los Angeles, left behind 280 km^2 of salty erodible land which become a major source of salty dust storm in the region.

As described in the given example cases, either climate change, anthropogenic changes, or a combination of both have been shown to be responsible for lake level and volume changes. These factors are however interconnected which means that they can accelerate each other's effect on the water balance of the basins. For instance, drier climate leads to higher demand of irrigation and water use, which accelerate the adverse effects of climate change. Present results for Lake Urmia show that both climate change and water diversions for irrigation are the main factors behind the observed lake area and volume reduction.

Since the LUDB is divided between three provinces, it is managed mainly at the provincial level with oversight at the national level, which means that a high degree of cooperation between the three provinces is needed in order to develop an integrated and sustainable water resource management plan. Such a plan should also be based on comprehensive studies. Thus freely accessible data of LUDB is a necessary first step for further studies on the water resources of the region.

Even without such comprehensive studies, several different regional plans have been proposed to deal with the Lake Urmia's crisis. Watershed management, decreasing the irrigation water, releasing the water behind dams to the main contributing rivers and importing water from neighboring basins are the most discussed solutions for the Lake

Urmia's crises (Abbaspour and Nazaridoust 2007, UNDP 2012, Henareh 2014, Eimanifar and Mohebbi, 2007).

The quickest solution is to release the volume of water stored in dam reservoirs. Based on the results of this study assuming the annual precipitation as the average of the last fifteen years over the lake, Lake Urmia needs 3.195 km^3 to stay in a steady. Abbaspour and Nazaridoust (2006) evaluate the necessary annual input flow to the lake in order to have a sustainable ecosystem as 3.086 km^3. The main problem with this solution is that the river flow has already affected by the periodic regional droughts, and irrigation in the basin is highly dependent on the river flow in the basin. Domestic water use also, is highly dependent on the operating dams. On the other hand according to IWR (2014) the total regulating volume of the operating dams at 2013 is approximately 2.0 km^3 that is only two-third of the needed water to compensate the evaporation over the lake.

More long-term solutions such as importing water from neighboring basins have considerable practical and environmental issues. Three main suggested water sources for this purpose are Caspian Sea, Aras River and Zab River (UNEP 2014). Beside the high cost and environmental consequences of transferring water, both rivers are the transboundary rivers. Water withdrawal from them may violate other neighboring countries' water right and lead to political conflicts with them. The other option, the Caspian see, with an average surface level 28 meters below the sea level is bordered by five countries including Iran (Leontiev 2014). The lowest water level of Lake Urmia, on the other hand is 1270.59 m above sea level. That means that a high amount of energy is needed to transfer water from the Caspian Sea to Lake Urmia. Besides that, the high mountain range of Alborz separates the two lakes. Crossing it may have significant costs and environmental consequences.

Instead of importing water and exporting problems to other places, the only reasonable solution seems to be integrated water management in the basin, including measures such as and water saving through more efficient irrigation systems, and choosing cropping suitable for the conditions of the basin.

5. Conclusions

In this study, the water balance model of the Lake Urmia Drainage Basin was developed. The only input to the closed basin was precipitation and the main outputs were evapotranspiration from the land and evaporation from the lake's surface. The annual precipitation, averaged using Thiessen polygon method, was 354 mm over the basin and 323 mm over the lake. The annual evapotranspiration over the basin was estimated at 287 mm using Turc-Langbein method. The annual evaporation over the lake was estimated using energy balance approach as 932 mm with a decreasing trend due to increase in the lake's salinity.

The annual water balance of the model was developed to simulate the Lake Urmia's water level given an estimated linear development of irrigated lands from 300000 ha to 500000 ha in the last three decades, which is consistent with the best available data on the actual irrigation development in the basin. The maximum error of the simulation was found to be 1.03 m, which corresponds to 6.4% of the maximum depth of 16 m and the RMSE of simulated water level relative to observed water level was 0.40 m i.e. 2.5% of maximum depth and 6.7% of mean depth.

Based on the results of this study, we conclude that the main factor driving the observed water level changes of Lake Urmia is the change in the precipitation over the lake's drainage basin since 1950. This could explain 62% of the observed lake level decrease. Irrigation developments during the last four decades were found to be responsible for 32% of the observed lake level decrease.

Thus the future of the water level of the Lake Urmia is very likely to continue to decrease unless the current climate condition will be followed by period of increased precipitation. If the current climate conditions will prevail also in the future, even a 20% decrease in the irrigated land area which is actually quite ambitious, will not make the lake recover to its ecological level at the end of 2020.

References

Abatzopoulos TJ, Agh N, Van Stappen G, Razavi Rouhani SM, Sorgeloos P (2006), *Artemia sites in Iran. J Mar Biol Ass*., 86:299-307.

Abbaspour M. & Nazaridoust, A., (2007). *Determination of environmental water requirement of Lake Urmia, Iran: an ecological approach*. International Journal of Environmental Studies, Volume 64 (2), pp. 161-169.

Abdusselam A, (2007), *Forecasting surface water level fluctuations of Lake Van by artificial neural networks*. Water Resour Manage 21:399–408

AghaKouchak Amir, Norouzi Hamid, Madani Kaveh, Mirchi Ali, Azarderakhsh Marzi, Nazemi Ali, Nasrollahi Nasrin, Farahmand Alireza, Mehran Ali, Hasanzadeh Elmira, (2014), *Aral Sea syndrome desiccates Lake Urmia: Call for action*, J. Great Lakes Res. available at: http://dx.doi.org/10.1016/j.jglr.2014.12.007

Aksoy H., Unal N. E. , Eris E. , and Yuce M. I. (2013) *Stochastic modeling of Lake Van water level time series with jumps and multiple trends*, Hydrol. Earth Syst. Sci., 17, 2297–2303,

Alipour, H., Ghasemi, H., Olya, T., (2014): *Sustainable planning model toward reviving Lake Urmia*, International Journal of Water Resources Development

Andreas P. Savva and Karen Frenken (2002), *Crop Water Requirements and Irrigation Scheduling, Irrigation Manual Module 4*. Food and Agricultural Organization of United Nations (FAO) . Available at : ftp://ftp.fao.org/docrep/fao/010/ai593e/ai593e00.pdf

Chow V. T., Maidment D. R., and Mays L.W.(1988), Applied Hydrology. McGraw-HillBook Co., New York. 1988.

Chunlan, L., Gaodi, X., Heqing, HUANG, (2006). *Shrinking and Drying up of Baiyangdian Lake Wetland: A Natural or Human Cause?* Chinese Geographical Science.16(4) 314–319

Cretaux, J. F. Letolle, R., Bergé-Nguyen M., *History of Aral Sea level variability and current scientific debates*, Global and Planetary Change, Volume 110, Part A, November 2013, Pages 99-113, ISSN 0921-8181

Dekker, D. (2014) *The Effect of Water Diversions and Drought in the Drying-up of Beaverhills Lake, a 140 km^2 Ramsar Wetland in Central Alberta*. Natural Areas Journal 34(3):346-352.

Destouni, G., S. M. Asokan, and J. Jarsjö (2010), Inland hydro-climatic interaction: Effects of human water use on regional climate, Geophys. Res. Lett., 37, L18402.

Detlef P. van Vuuren & Jae Edmonds & Mikiko Kainuma & Keywan Riahi & Allison Thomson & Kathy Hibbard & George C. Hurtt & Tom Kram & Volker Krey & Jean-Francois Lamarque & Toshihiko Masui & Malte Meinshausen & Nebojsa Nakicenovic & Steven J. Smith & Steven K. Rose (2011), *The representative concentration pathways: an overview*. Climatic Change 109:5–31.

Dingman, S. L., (2002), *Physical Hydrology*, 2nd Edition, Prentice- Hall, New Jersey USA.

Eimanifar, A. & Mohebbi, F.,(2007). *Urmia Lake (Northwest Iran): a brief review*. *Saline Systems*, 3(5)

Food and Agriculture Organization of the United Nations, FAO (2014) aquastat : http://www.fao.org/nr/water/aquastat/globalmaps/index.stm

Ghaheri, M., Baghal-Vayjooee, M., Naziri, J., 1999. Lake Urmia, Iran: a summary review. Int. J. Salt Lake Res. 8 (1), 19–22.

Hassanzadeh E., Zarghami M., Hassanzadeh, Y., (2011). *Determining the Main Factors in Declining the Urmia Lake Level by Using Dynamics Modeling*, Water Resources Management, Volume 26(1), pp. 129-145

Henareh, K. A., Mayer, A. L., Norman, E. S. (2014) Water Flows Toward Power: Socioecological Degradation of Lake Urmia, Iran, Society & Natural Resources: An International Journal, 27:7, 759-767

Iran's Meteorological Organization, IRIMO (2014), Iran's synoptic weather station data: http://www.chaharmahalmet.ir/iranarchive.asp

Iranian Water Resources Management Company, IWR (2014), *Iran dams* : http://daminfo.wrm.ir/fa/tabularview?rnd=51407

Jarvis, A., H.I. Reuter, A. Nelson, E. Guevara, 2008, *Hole-filled SRTM for the globe Version 4*, available from the CGIAR-CSI SRTM 90m Database: http://srtm.csi.cgiar.org.

Karbassi, A., Nabi Bidhendi, G., Pejman, A. & Esmaeili Bidhendi, M., 2010. *Environmental Impacts of Desalination on the Ecology of Lake Urmia*, Journal of Great Lakes Research, Volume 36(3), pp. 419-424.

Leontiev. O. K. (2014), Caspian Sea. Encyclopedia Britannica, available at: http://global.britannica.com/EBchecked/topic/98044/Caspian-Sea#a-gigya-comments

McCutcheon, S.C., Martin, J.L, Barnwell, T.O. Jr. 1993, *Handbood of Hydrology*, McGraw-Hill, New York, NY p. 11.3

Mohammadi, M. A. (2005), *Relation between evaporation in saline waters and in fresh water and its effect on Lake Urmia's evaporation*, West Azerbaijan regional water authority's report. Available at: http://www.wrm.ir/rwrd/AG001_final.pdf

American National Aeronautics and Space Administration, NASA (2015),Worldview. Available at: https://earthdata.nasa.gov/labs/worldview/

Nasiri Ali, (2003) *Mapping the environmental land use in the ecological zone of the Lake Urmia using GPS and ETM data*. Iran's Ministry of Agriculture Jihad, Report 81/03, Available at: (http://www.maj.ir/portal/File/ShowFile.aspx?ID=f59ba78e-fd40-4d32-91ca-08b6ff5eaf3d).

Numerical Terradynamic Simulation Group, NTSG (2014), Modis : http://www.ntsg.umt.edu/project/modis

Reheis, M. C. (1997), *Dust deposition downwind of Owens (dry) Lake, 1991–1994: Preliminary findings*, J. Geophys. Res., 102(D22), 25999–26008.

Salhotra A. M., Adams. E. E. and Harleman D. R. F., (1985), *Effect of Salinity and Ionic Composition on Evaporation: Analysis of Dead Sea Evaporation Pans*, Water Resources Research, vol. 21, no. 9, 1336-134.

Shibuo, Y., Jarsjö, J., Destouni, G., 2007. *Hydrological responses to climate change and irrigation in the Aral Sea drainage basin*. Geophysical Research Letters 34.

Sima S., Ahmadalipour A., Tajrishy M. (2013), *Mapping surface temperature in a hyper-saline lake and investigating the effect of temperature distribution on the lake evaporation*, Remote Sensing of Environment 136, 374–385.

Sima S., Tajrishy M. (2013), *Using satellite data to extract volume–area–elevation relationships for Urmia Lake, Iran*. Journal of Great Lakes Research 39, 90–99.

Solubility Table, (2014) Retrieved October 23 2014, available at: http://en.wikipedia.org/wiki/Solubility_table

The Ramsar Sites Information Service,(2014), Ramsar Site List. Accessed august 15 2014 at: https://rsis.ramsar.org/ris/38?language=en

Törnqvist. R., Jarsjö. J., (2012), *Water Savings Through Improved Irrigation Techniques: Basin-Scale Quantification in Semi-Arid Environments.* Water Resources Management, Volume 26, Issue 4, pp 949-962

Urmia Lake Restoration Program, ULRP (2014), Urmia Lake Restoration Program committee: http://ulrp.sharif.ir/

United Nations Environment Programme, UNEP, 2012. *The drying of Iran's Lake Urmia and its environmental consequences*. Tech. rep. United Nations Environment Programme (UNEP) Global Environmental Alert Service (GEAS).

United Nations Population Fund, UNFPA (2014), United Nations Population Fund in Iran, available at: http://iran.unfpa.org/Country%20Profile.asp

United States Geological Survey, USGS (2014), Landsat, available at: http://landsatlook.usgs.gov/viewer.html

Waiser M.J. and Robarts R.D., Saline Inland Waters, In Encyclopedia of Inland Waters, edited by Gene E. Likens, Academic Press, Oxford, 2009, Pages 634-644,

Yin X., Nicholson SH, (1998), *The water balance of Lake Victoria*, Hydrological Sciences Journal, 43:5, 789-811.

Zeinoddini, M., Tofighi, M., Vafaee, F. (2009). *Evaluation of dike-type causeway impacts on the flow and salinity regimes in Urmia Lake, Iran*. Journal of Great Lakes Research, 35(1), 13-22

Appendix A

A.1 Water balance of a Lake

All inflows and outflows need to be determined in order to estimate the change of lake storage. Considering a net change over a year, this can be expressed as:

$$\Delta S = V_{in} - V_{out} \qquad \text{(A-1)}$$

where ΔS, is the change in the storage volume [L^3] over a year, and V_{in} and V_{out} are the annual volume of the inflow and outflow [L^3] respectively. Considering the water fluxes in a drainage basin assuming all water fluxes end up or start from the basin's reservoir, the equation (2-1) can be re-written as equation (2-2):

$$\Delta S = P + SW_{in} + GW_{in} - SW_{out} - GW_{out} - ETa_{basin} - E_{lake} \qquad \text{(A-2)}$$

where, P is the annual precipitation over the drainage basin and lake [L^3], SW_{in} and SW_{out} are the annual surface water inflow and outflow respectively, GW_{in} and GW_{out} are the annual groundwater inflow and outflow respectively [L^3], Eta_{basin} is the actual evapotranspiration from the drainage basin [L^3] and E_{lake} is the evaporation from the water bodies in the basin [L^3].

In the Lake Urmia's closed drainage basin surrounded by high mountains, with no known major groundwater fluxes into or from adjacent basins, the major input to the basin is precipitation. The only known outputs from the basin are evaporation from the lake and other water bodies in the catchment, and evapotranspiration over the catchment terrain. Because of the small area of other water bodies (i.e. dams and wetlands) relative to the Lake Urmia's surface area, we will in the following neglect evaporation from the water bodies in the catchment. Thus the annual water balance equation of the Lake Urmia can then be re-written as equation (A-3):

$$\Delta S = P_{basin} - ETa_{basin} + P_{lake} - E_{lake} \qquad \text{(A-3)}$$

where, P_{basin} and P_{lake} are the P over the drainage basin and the lake respectively.

A.2 Evapotranspiration

The actual evapotranspiration (Eta_{basin}) was estimated as a function of ETp. Langbein (1949) introduced a model to estimate the annual ETp based on only average annual temperature:

$$ETp = 325 + 21T + 0.9T^2 \qquad \text{(A-4)}$$

Where, ETp is the annual potential evapotranspiration (mm) and T is the average annual Temperature over the land (°C). Then ETa_{basin} can be estimated using a model introduced by Turc (1954) as a function of available water, precipitation, and the:

$$ETa_{basin} = \frac{P_{basin}}{\sqrt{0.9 + \frac{P^2_{basin}}{ETp^2}}} \quad \text{(A-5)}$$

Recently remote sensing based approaches have been developed to estimate ETa_{basin}. For instance using NASA satellite data, Moderate Resolution Imaging Spectroradiometer (MODIS), The Numerical Terradynamic Simulation Group (NTSG) at the University of Montana, provide the global monthly evapotranspiration (NTSG 2014) which in this study was used as independent source to verify the results of Turc-Langbein method.

A.1. Evaporation

Since the evaporation is the main output from Lake Urmia, estimation of the evaporation over the lake with acceptable accuracy is of great interest. Evaporation over free water or a lake can be either directly estimated using a pan-evaporation measurement, or modeled using energy flux and atmospheric data. Lack of direct evaporation measurement, however, is a main challenge in most of the cases. But even a short period of direct measurement data can be a helpful tool to verify the results of other indirect methods.

A.1.1 Pan-Evaporation approach

In a Pan-evaporation approach, water loss in a cylindrical pan filled with liquid water exposed to atmosphere is measured, and then the pan evaporation can be calculated using a simple water balance equation (equation A-6):

$$Ep = P - (V_2 - V_1) \quad \text{(A-6)}$$

here, Ep is the evaporation from the pan during the time period ($\Delta t = t_2 - t_1$), P is the precipitation during the time period Δt and V_2 and V_1 are the pan water volume at the time t_2 and t_1 respectively. Then free water evaporation can be calculated as a portion of the Ep as following:

$$E = k_p \cdot Ep \quad \text{(A-7)}$$

where, k_p is the pan coefficient which is (0.7-0.8) for the Class-A pan (Chow et al. 1988). These values are for fresh water, but since the evaporation decrease with increase in the salinity of water, an addition multiplier is needed to estimate the evaporation of saline water (Salhotra et al. 1985). Thus the evaporation of saline water can be estimated using equation (2-8).

$$E = \Theta \cdot k_p \cdot Ep \quad \text{(A-8)}$$

Where, Θ ($0 \leq \Theta \leq 1$) is a ratio of evaporation of saline water to the evaporation of freshwater.

A.1.2 Energy Balance approach

In the cases where direct measurement of evaporation is either not available or available only for limited periods of time, mathematical models – analytical or empirical - can be helpful.

One of the widely used methods to estimate evaporation over a lake is the energy balance approach which we adopt in this work the general energy balance of an evaporating water body can be described as equation (A-9):

$$\frac{\Delta Q}{\Delta t} = K + L - G - H + A_w - LE \qquad \text{(A-9)}$$

here, the left side is change in the stored energy of the system, *ΔQ*, during the time period of *Δt* and the right side is the net energy flux of the system via shortwave radiation, K; longwave radiation, L; conduction to the ground, G; sensible heat exchange with atmosphere, H; water- advected energy, Aw and evaporation, LE.

To simplify the equation (A-9), it is useful to use the ratio of sensible heat exchange to latent heat exchange, defined by Bowen (1926):

$$B = H / LE \qquad \text{(A-10)}$$

In which the Bowen ratio is defined as (Bowen 1926):

$$B = \frac{c_a \cdot P}{(0.622 \cdot \lambda v)} \cdot \frac{(T_s - T_a)}{(e^* - e)} \qquad \text{(A-11)}$$

in which, c_a is the heat capacity of the air ($c_a = 1.00 \times 10^{-3}$ MJkg^{-1}K^{-1}), P is atmospheric pressure in Kpa, T_s and T_a are water surface and atmosphere temperature respectively and e* and e, are saturation and air vapor pressure respectively, which can be calculated as following:

$$e_s^* = 0.611 \cdot \exp\left(\frac{17.3 \cdot T_s}{T_s + 237.3} \right) \qquad \text{(A-12)}$$

here, vapor pressure is in Kpa and temperature in °C. Air saturation vapor pressure, e_a^*, can be calculated using equation (A-12) by using air temperature T_a instead. Then air vapor pressure is defined by:

$$e_a = W_a \cdot e_a^* \qquad \text{(A-13)}$$

in which, W_a is relative humidity.

Latent heat exchange, *LE* [EL^{-2}T^{-1}] can be calculated as:

$$LE = \rho_w \cdot \lambda_v \cdot E \qquad \text{(A-14)}$$

where E is evaporation, ρ_w is water mass density and λ_v, is the latent heat of vaporization which can be calculated as:

$$\lambda_v = 2.50 - 2.36 \times 10^{-3} T_s \qquad \text{(A-15)}$$

where λ_v is in $MJkg^{-1}$ and T_s is water surface temperature in °C.

In the annual based balance, the change in the stored energy of the system, *ΔQ*, the conduction to the ground, G; and water- advected energy, Aw, can be neglected (Yin and Nicholson 1998). Thus combining the equation (A-9), (A-10) and (A-14), evaporation can be calculated as:

$$E = \frac{K + L}{\rho_w \cdot \lambda v \cdot (1 + B)} \qquad \text{(A-16)}$$

The net input shortwave (solar) radiation is defined as:

$$K = K_{in} \cdot (1 - \alpha) \qquad \text{(A-17)}$$

where α is albedo or reflectivity of water and K_{in} is the incoming solar radiation in $MJm^{-2}day^{-1}$ that can be calculated using the empirical equation provided by Croley (1989) as following (Dingman 2002):

$$K_{in} = \left(0.355 + 0.68 \cdot (1 - C)\right) \cdot K_{cs} \qquad \text{(A-18)}$$

where, K_{cs} is the total daily clear sky radiation incident on a horizontal plane and C is cloudiness. The detailed procedures of calculation of K_{cs}, is given in Appendix B.
Albedo of water surface can be estimated using empirical model of Koberg (1964) as function of K_{in} (Dingman 2002):

$$\alpha = 0.127 \cdot \exp(-0.0258 \cdot K_{in}) \qquad \text{(A-19)}$$

here, K_{in} is in $MJm^{-2}day^{-1}$.

Longwave radiation is defined as:

$$L = \varepsilon_w \cdot \varepsilon_{at} \cdot \sigma \cdot (T_a + 273.2)^4 - \varepsilon_w \cdot \sigma \cdot (T_s + 273.2)^4 \qquad \text{(A-20)}$$

where, L is the long wave radiation in $MJm^{-2}day^{-1}$, σ is the Stephan-Boltzmann constant ($\sigma = 4.90 \times 10^{-9}$ $MJm^{-2}day^{-1}$ K^{-4}), ε_w is the emissivity of the water surface ($\varepsilon_w = 0.97$) and ε_{at} is the effective emissivity of the atmosphere which can be calculated by equation (A-21):

$$\varepsilon_{at} = 1.72 \cdot \left(\frac{e_a}{T_a + 273.2}\right)^{1/7} \cdot (1 + 0.22 \cdot C^2) \qquad \text{(A-21)}$$

where, T_{at} is the atmosphere temperature.

Appendix B

B.1. Daily Clear-Sky Solar Radiation on a Horizontal Plane

Solar radiation is an important component in study of the energy balance at the earth's surface. But since it is not measured widely, it is useful to estimate it based on other more available measured data. Here, the astronomic relations developed by Iqbal (1983) are used to estimate the solar radiation incident at the top of atmosphere, thereby, estimate the clear-sky solar radiation on a horizontal plane (Dingman 2002).

Here is some astronomical relation and definitions that is used in the calculation process:

B.1.1. Solar constant

The average radiation flux at the upper surface of atmosphere is called solar constant ($I_{sc} =$ 4.921 $MJm^{-2}hr^{-1}$).

B.1.2. Day angle

Day angle which is the position of the earth on its orbit around sun is given by:

$$\Gamma = \frac{2 \times \pi \times (J - 1)}{365} \quad \text{(B-1)}$$

In which J is the day number, (1≤J≤365) which start at the 1 January and ends at 31 December.

B.1.3. Eccentricity

Eccentricity in any time is the square of the ratio of the average distance between the sun and the planet earth to their distance at any time which can be calculated by equation (B.2)

$$\begin{aligned} E_0 = {} & 1.000110 + 0.034221 \times \cos(\Gamma) + 0.001280 \times \sin(\Gamma) \\ & + 0.000719 \times \cos(2\Gamma) + 0.000077 \times \sin(2\Gamma) \end{aligned} \quad \text{(B-2)}$$

B.1.4. Declination

Latitude of the sun at noon is called declination which is calculated as:

$$\begin{aligned} \delta = {} & (180/\pi)\ [0.006918 - 0.399912 \times \cos(\Gamma) + 0.070257 \\ & \times \sin(\Gamma) - 0.006758 \times \cos(2\Gamma) + 0.000907 \times \sin(2\Gamma) \\ & - 0.002697 \times \cos(3\Gamma) + 0.00148 \times \sin(3\Gamma)] \end{aligned} \quad \text{(B-3)}$$

Here the declination is in degree.

B.1.5. Sunrise

Sunrise is the time of sunrise before noon in hours. The length of the day can be calculated by absolute value of the sun rise by 2.

$$T_{hr} = \frac{-\cos^{-1}\left(-\tan(\delta)\times\tan(\Lambda)\right)}{w} \qquad \text{(B-4)}$$

Here Λ is latitude and w is the angular velocity of the earth's rotation. ($w = 15^{o}\,hr^{-1}$)

Daily solar radiation flux on horizontal plane

$$K_{ET} = 2\,I_{sc}\cdot E_0\cdot(\cos(\delta)\cdot\cos(\Lambda)\cdot\sin(w\cdot T_{hr})\;/(w) \\ +\sin(\delta)\cdot\sin(\Lambda)\cdot T_{hr}] \qquad \text{(B-5)}$$

B.1.6. Total daily clear sky radiation incident on a horizontal plane

Total daily clear sky radiation incident on a horizontal plane can be calculated as:

$$K_{cs} = \left(\tau+0.5\cdot\gamma_s\cdot\alpha\cdot\tau+0.50.5\cdot\gamma_s+0.25\cdot\gamma_s^{\,2}\cdot\alpha\right)\cdot K_{ET} \qquad \text{(B-6)}$$

Here, α is Albedo, τ is the total atmospheric transmissivity that is defined as:

$$\tau = \tau_{sa} - \gamma_{dust} \qquad \text{(B-7)}$$

Where:

$$\tau_{sa} = \exp\left(a_{sa} + b_{sa}\cdot M_{opt}\right) \qquad \text{(B-8)}$$

where

$$a_{sa} = -0.124 - 0.0207\cdot W_p \qquad \text{(B-9)}$$

And

$$b_{sa} = -0.0682 - 0.0248\cdot W_p \qquad \text{(B-10)}$$

In which, M_{opt} is the average daily optical air mass which can be estimated from figure (B-1), and W_p is precipitable-water content which can be calculated as:

$$b_{sa} = -0.0682 - 0.0248\cdot W_p \qquad \text{(B-11)}$$

Here T_d is dew point in °C.

And γ_s is attenuation of the solar beam due to scattering by water vapor and and permanent atmospheric constituent which is calculated as:

$$\gamma_s = \tau_s - \gamma_{dust} \quad \text{(B-12)}$$

Where

$$\tau_s = \exp\left(a_s + b_s \cdot M_{opt}\right) \quad \text{(B-13)}$$

Here

$$a_s = -0.0363 - 0.0084 \cdot W_p \quad \text{(B-14)}$$

And

$$b_s = -0.0572 - 0.0173 \cdot W_p \quad \text{(B-15)}$$

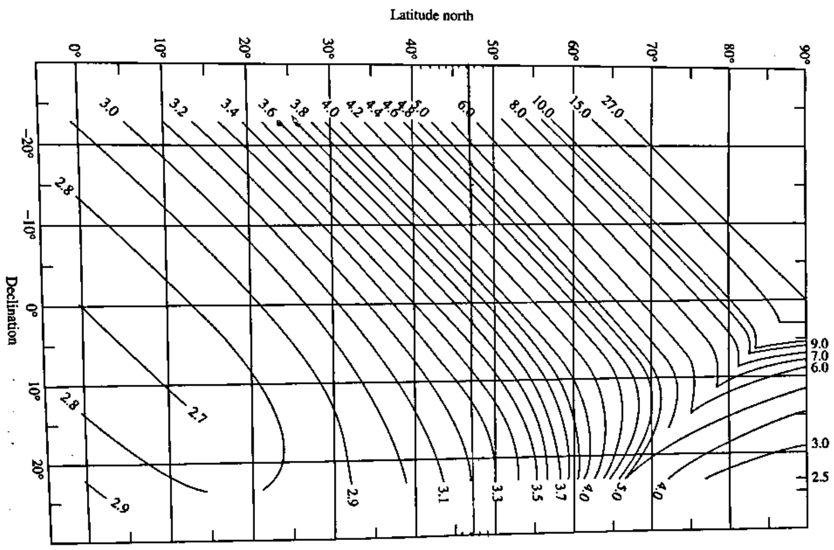

Figure B.1. Average daily optical air mass as function of latitude and declination for northern hemisphere by Kennedy (1940) after Dingman (2002)

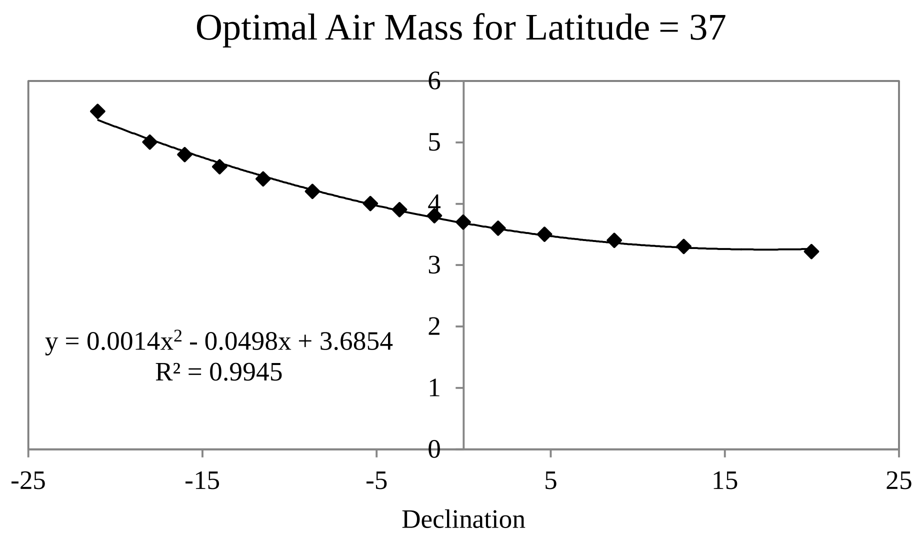

Figure A-2. Average daily optical air mass as a function of declination for latitude of 37

Appendix C

C.1. Precipitation missing data

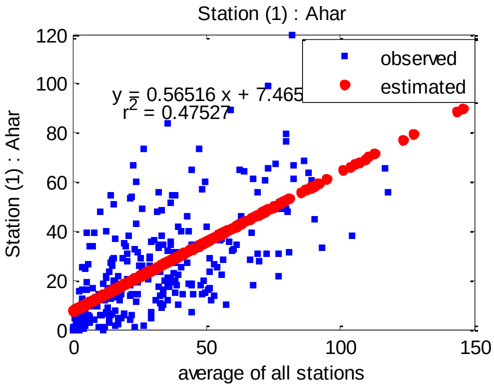

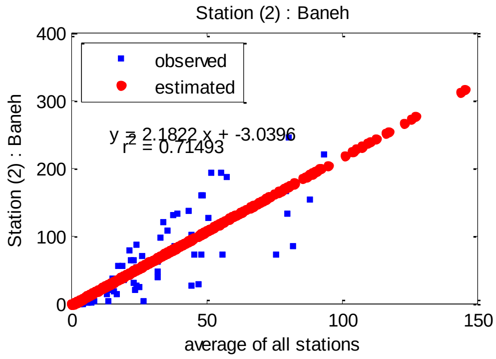

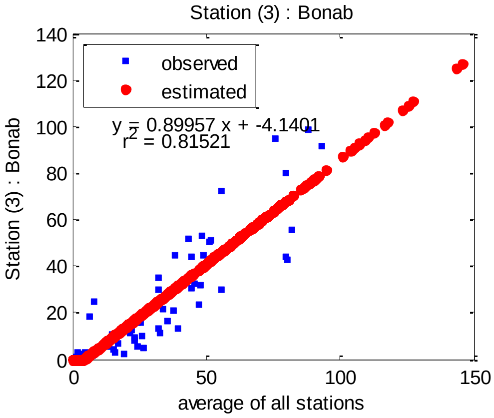

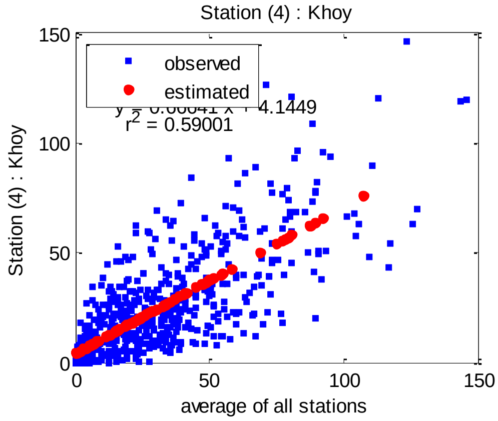

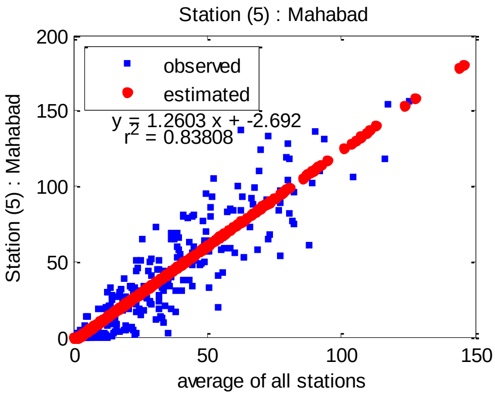

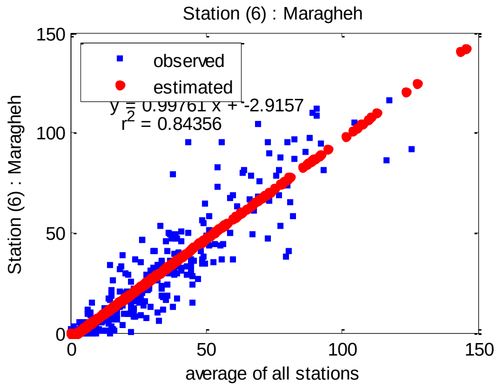

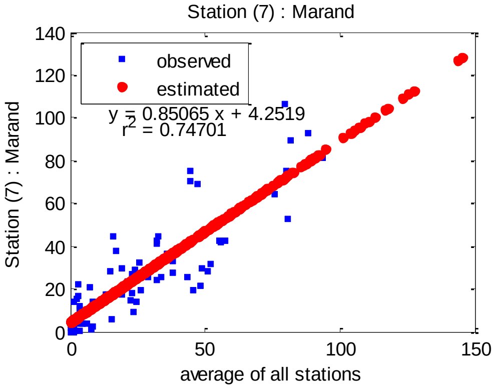

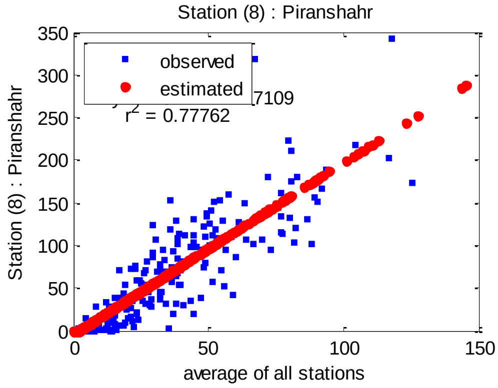

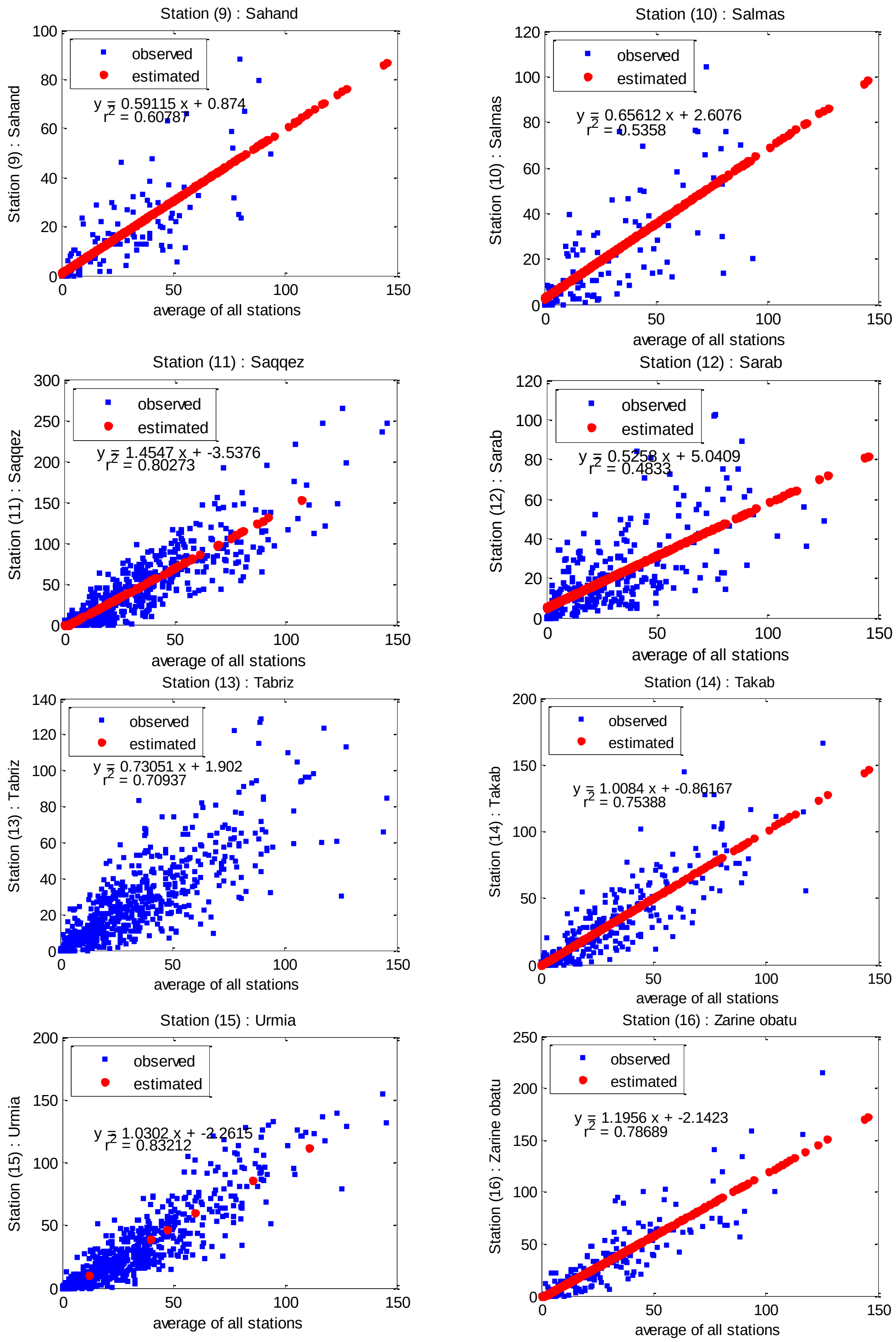
Station (9) : Sahand
observed
estimated
y = 0.59115 x + 0.874
r2 = 0.60787
Station (9) : Sahand
average of all stations
Station (10) : Salmas
observed
estimated
y = 0.65612 x + 2.6076
r2 = 0.5358
Station (10) : Salmas
average of all stations
Station (11) : Saqqez
observed
estimated
y = 1.4547 x + -3.5376
r2 = 0.80273
Station (11) : Saqqez
average of all stations
Station (12) : Sarab
observed
estimated
y = 0.5258 x + 5.0409
r2 = 0.4833
Station (12) : Sarab
average of all stations
Station (13) : Tabriz
observed
estimated
y = 0.73051 x + 1.902
r2 = 0.70937
Station (13) : Tabriz
average of all stations
Station (14) : Takab
observed
estimated
y = 1.0084 x + -0.86167
r2 = 0.75388
Station (14) : Takab
average of all stations
Station (15) : Urmia
observed
estimated
y = 1.0302 x + -2.2615
r2 = 0.83212
Station (15) : Urmia
average of all stations
Station (16) : Zarine obatu
observed
estimated
y = 1.1956 x + -2.1423
r2 = 0.78689
Station (16) : Zarine obatu
average of all stations

C.2. Temperature missing data

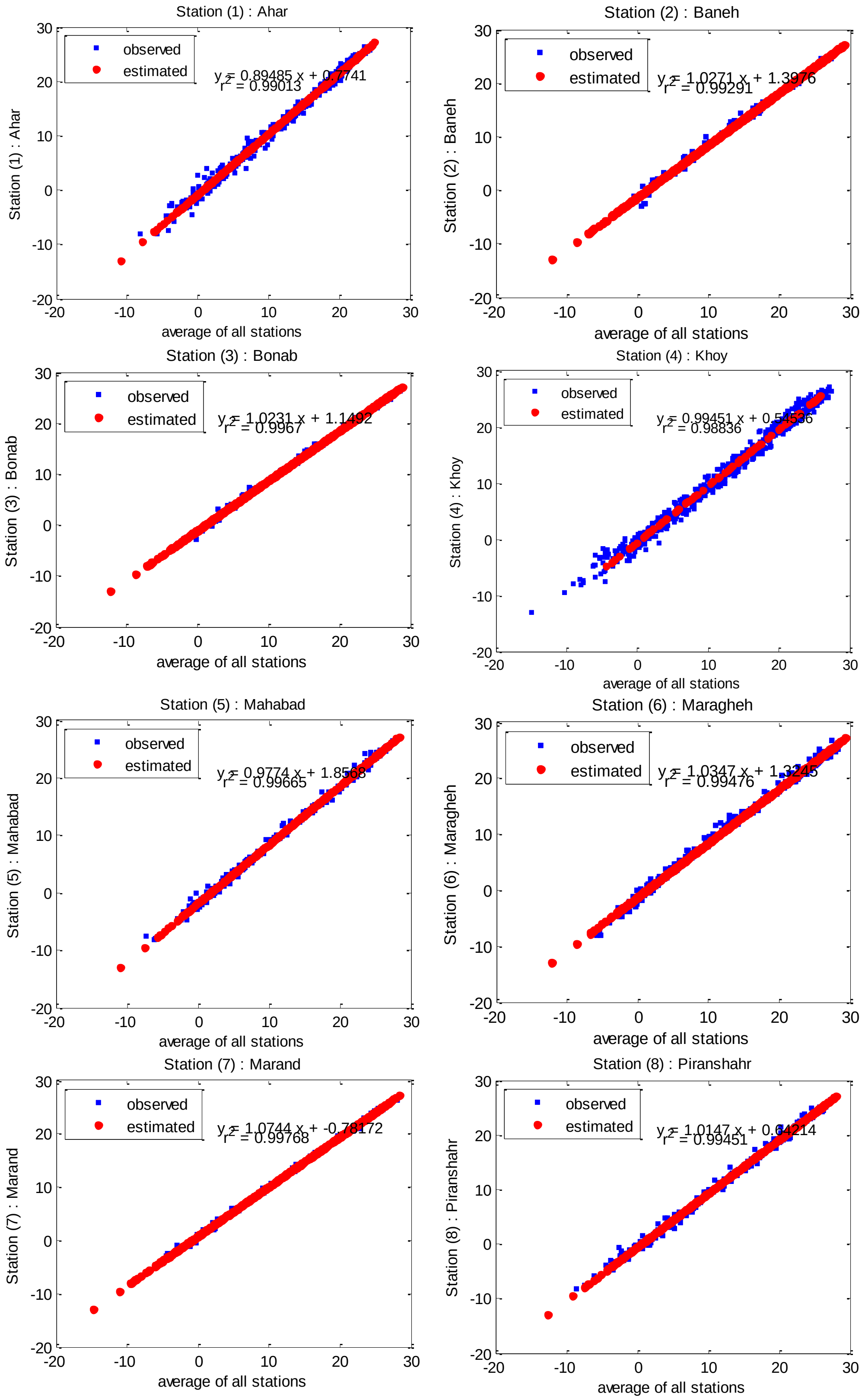

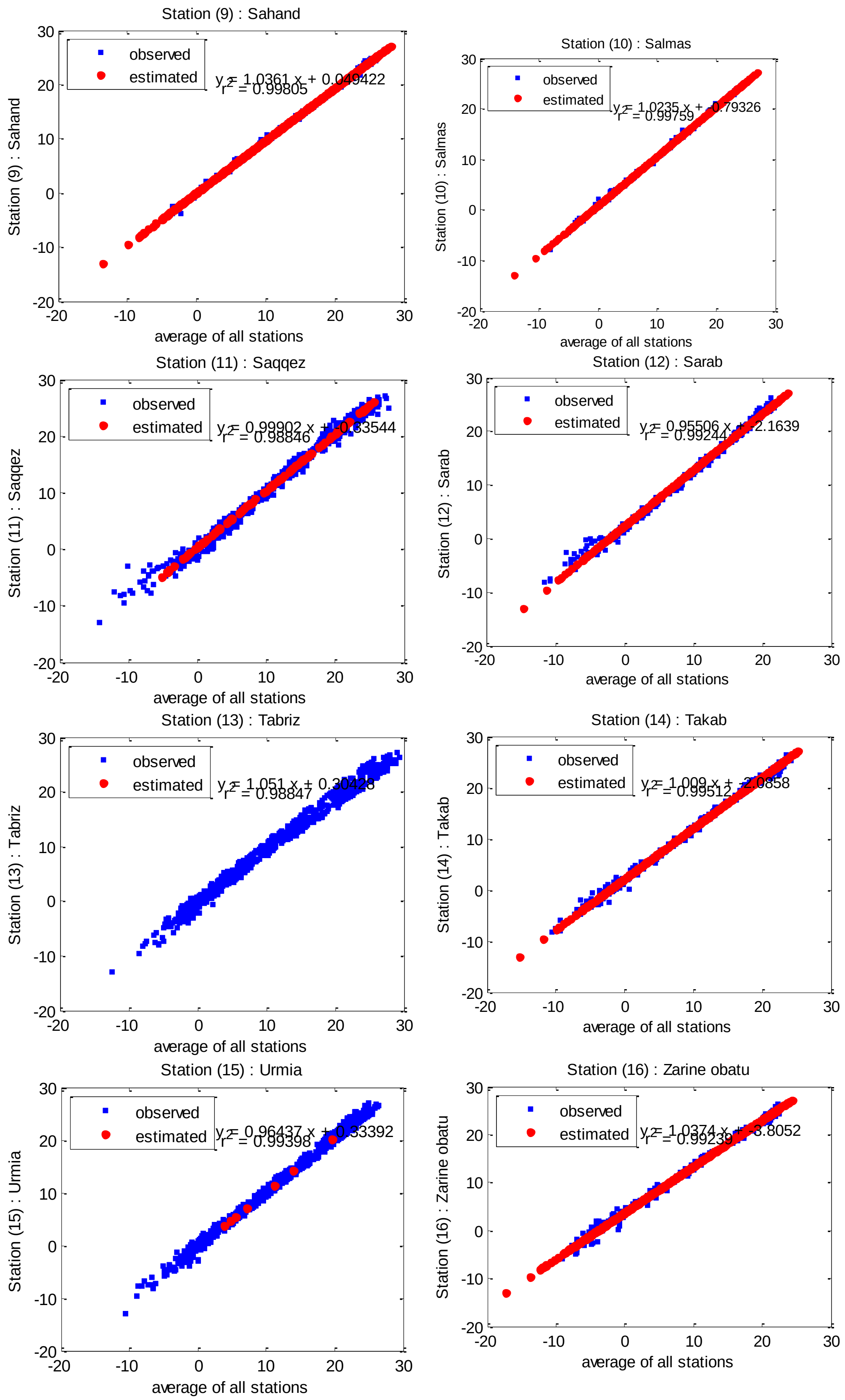
Station (9) : Sahand
observed
estimated
y = 1.0361 x + 0.049422
r² = 0.99805
Station (9) : Sahand
average of all stations
Station (10) : Salmas
observed
estimated
y = 1.0235 x + 0.79326
r² = 0.99759
Station (10) : Salmas
average of all stations
Station (11) : Saqqez
observed
estimated
y = 0.99902 x + 0.83544
r² = 0.98846
Station (11) : Saqqez
average of all stations
Station (12) : Sarab
observed
estimated
y = 0.95506 x + 2.1639
r² = 0.99244
Station (12) : Sarab
average of all stations
Station (13) : Tabriz
observed
estimated
y = 1.051 x + 0.30428
r² = 0.98847
Station (13) : Tabriz
average of all stations
Station (14) : Takab
observed
estimated
y = 1.009 x + 2.0858
r² = 0.99512
Station (14) : Takab
average of all stations
Station (15) : Urmia
observed
estimated
y = 0.96437 x + 0.33392
r² = 0.99398
Station (15) : Urmia
average of all stations
Station (16) : Zarine obatu
observed
estimated
y = 1.0374 x + 3.8052
r² = 0.99239
Station (16) : Zarine obatu
average of all stations

C.3. Relative humidity missing data

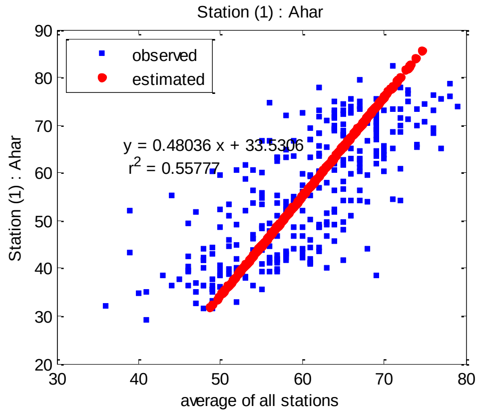

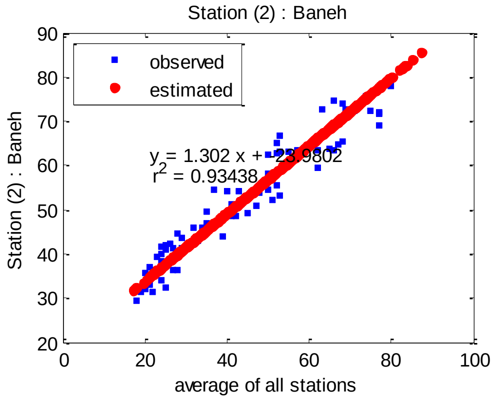

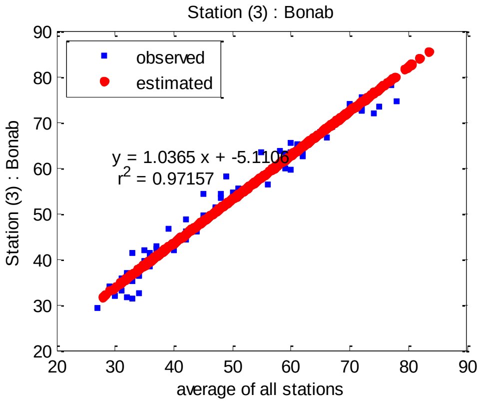

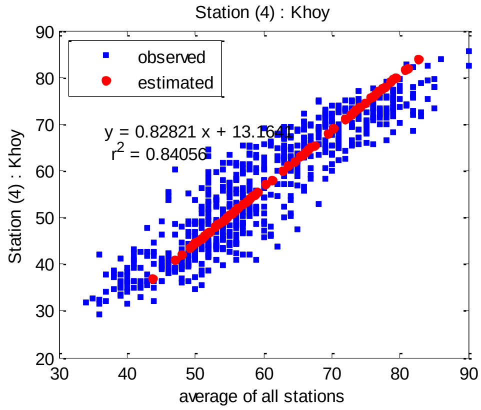

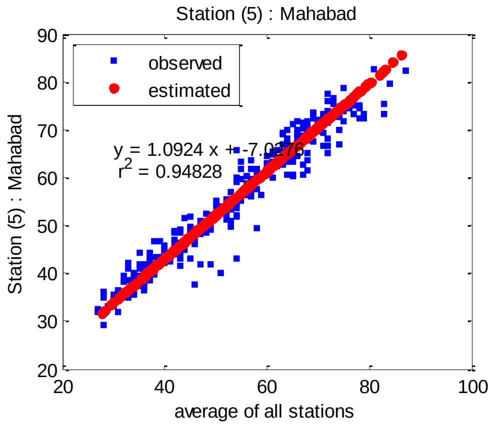

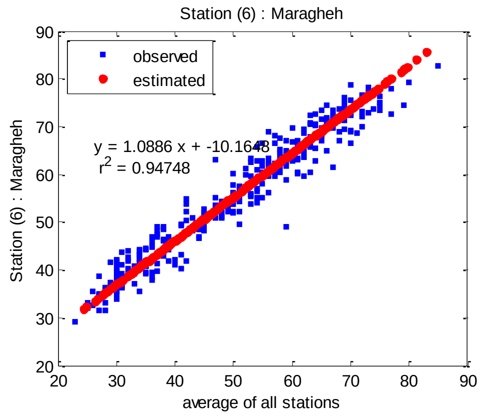

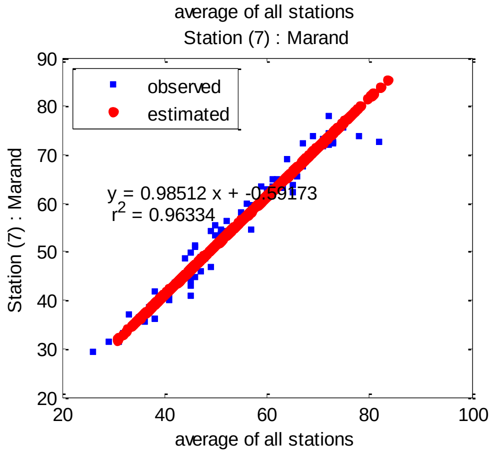

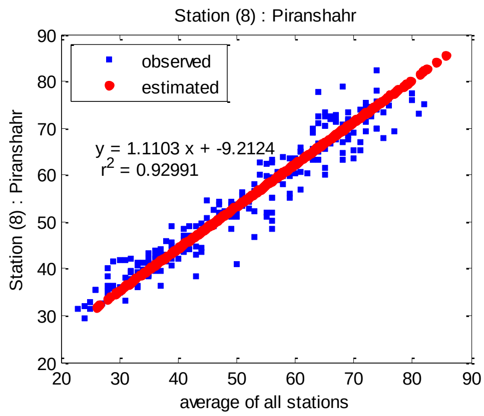

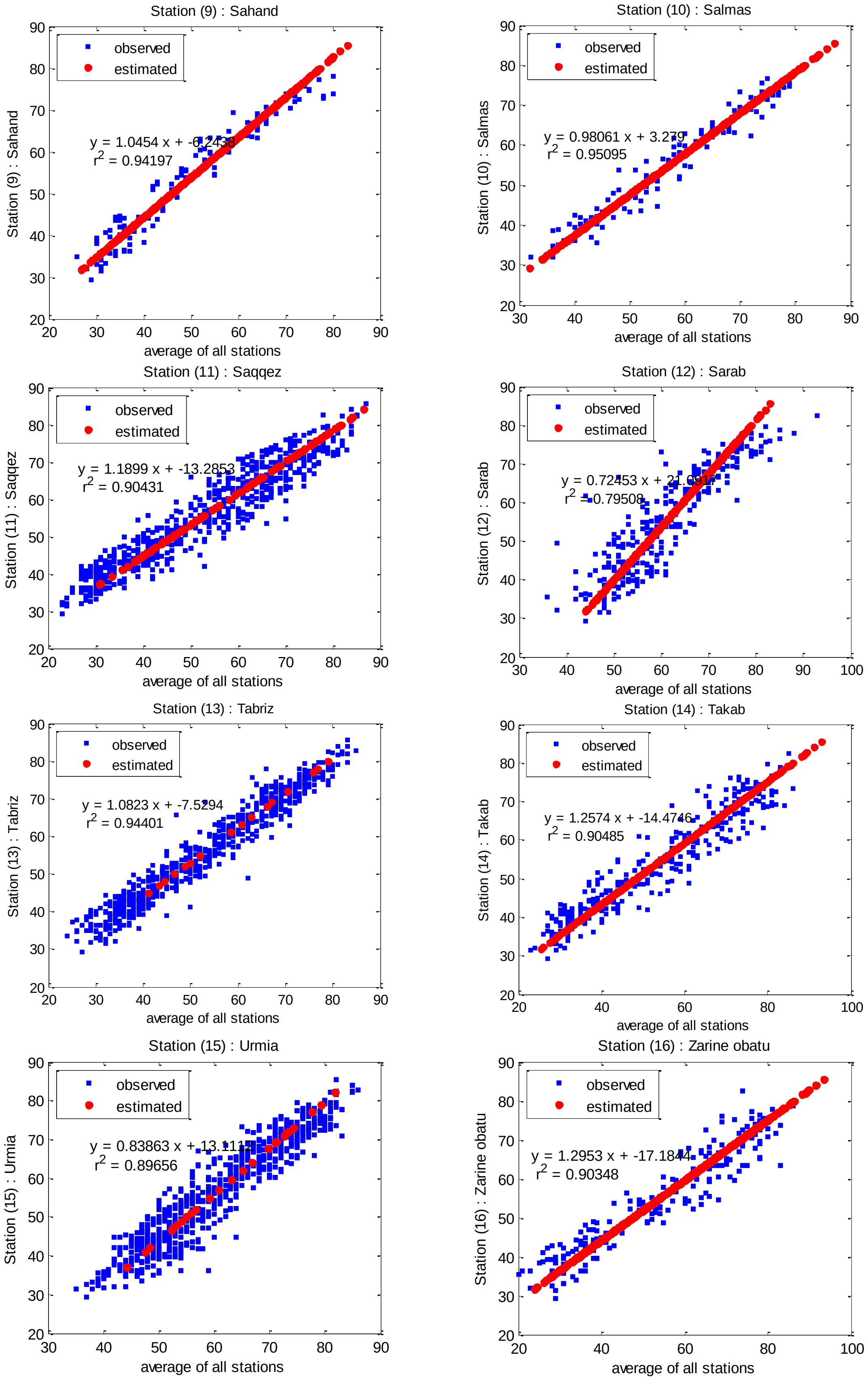
Station (9) : Sahand
observed
estimated
y = 1.0454 x + -6.2438
r2 = 0.94197
Station (9) : Sahand
average of all stations
Station (10) : Salmas
observed
estimated
y = 0.98061 x + 3.279
r2 = 0.95095
Station (10) : Salmas
average of all stations
Station (11) : Saqqez
observed
estimated
y = 1.1899 x + -13.2853
r2 = 0.90431
Station (11) : Saqqez
average of all stations
Station (12) : Sarab
observed
estimated
y = 0.72453 x + 21.0917
r2 = 0.79508
Station (12) : Sarab
average of all stations
Station (13) : Tabriz
observed
estimated
y = 1.0823 x + -7.5294
r2 = 0.94401
Station (13) : Tabriz
average of all stations
Station (14) : Takab
observed
estimated
y = 1.2574 x + -14.4746
r2 = 0.90485
Station (14) : Takab
average of all stations
Station (15) : Urmia
observed
estimated
y = 0.83863 x + 13.1112
r2 = 0.89656
Station (15) : Urmia
average of all stations
Station (16) : Zarine obatu
observed
estimated
y = 1.2953 x + -17.1844
r2 = 0.90348
Station (16) : Zarine obatu
average of all stations

C.4. Sunshine hours missing data

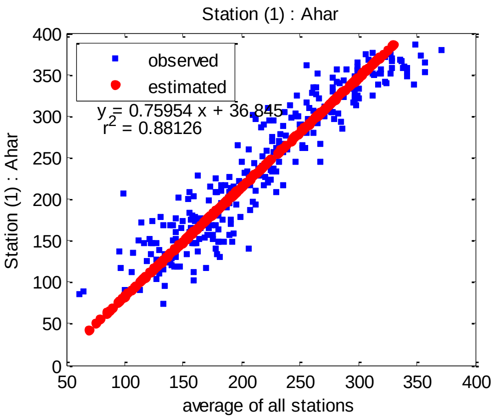

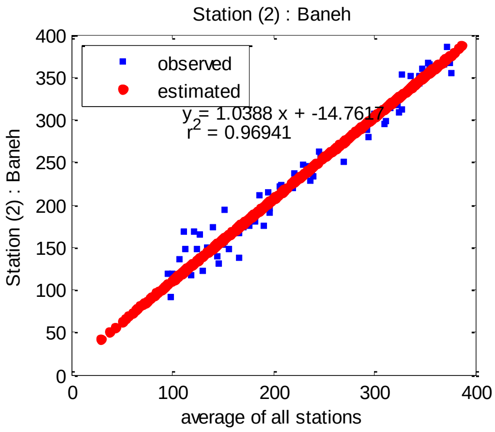

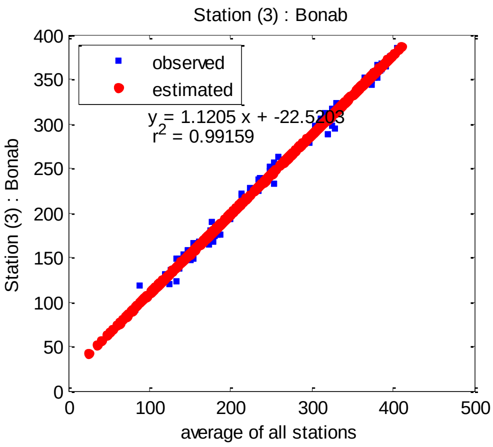

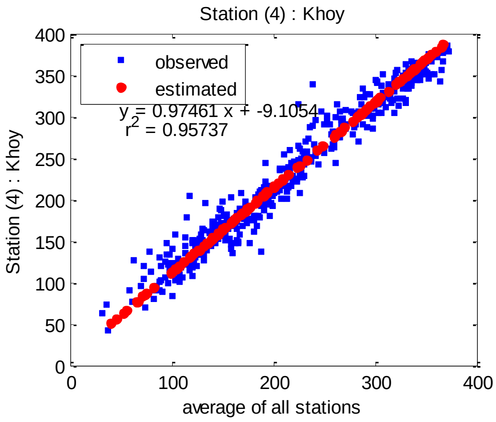

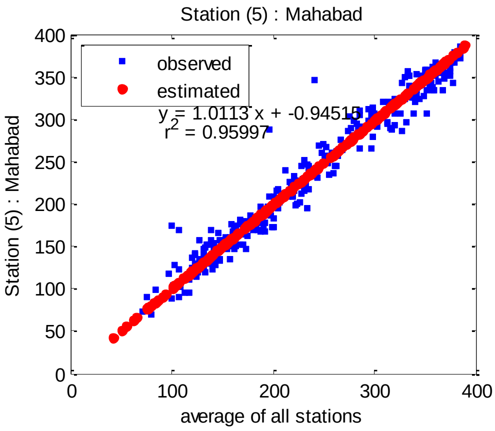

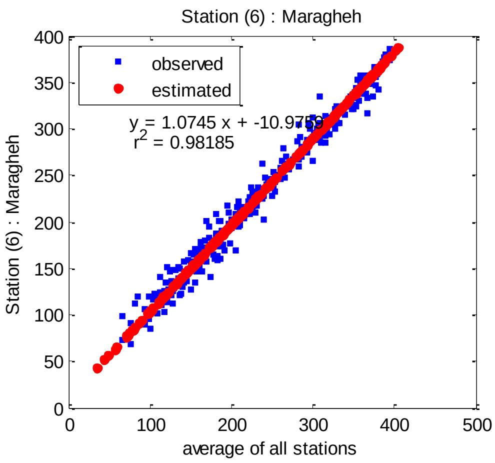

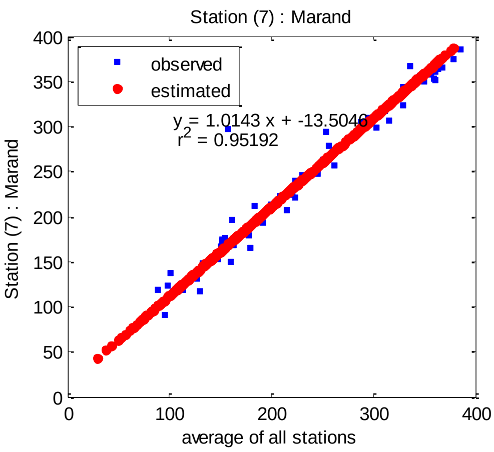

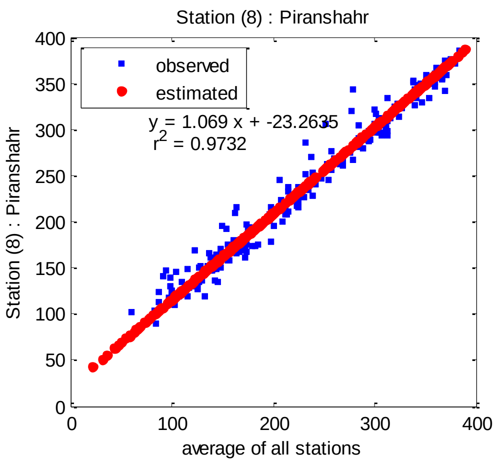

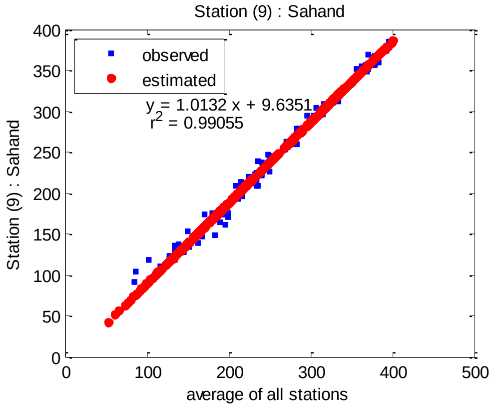
Station (9) : Sahand
observed
estimated
y = 1.0132 x + 9.6351
r2 = 0.99055
Station (9) : Sahand
average of all stations

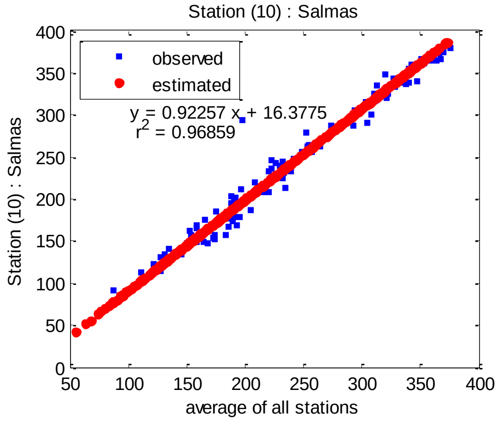
Station (10) : Salmas
observed
estimated
y = 0.92257 x + 16.3775
r2 = 0.96859
Station (10) : Salmas
average of all stations

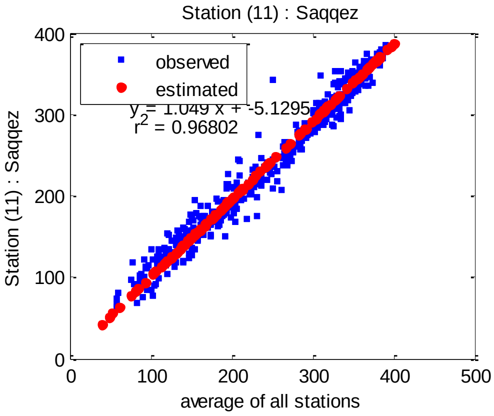
Station (11) : Saqqez
observed
estimated
-5.1295
r2 = 0.96802
Station (11) : Saqqez
average of all stations

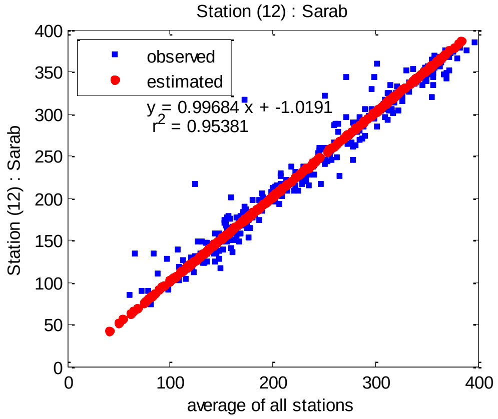
Station (12) : Sarab
observed
estimated
y = 0.99684 x + -1.0191
r2 = 0.95381
Station (12) : Sarab
average of all stations

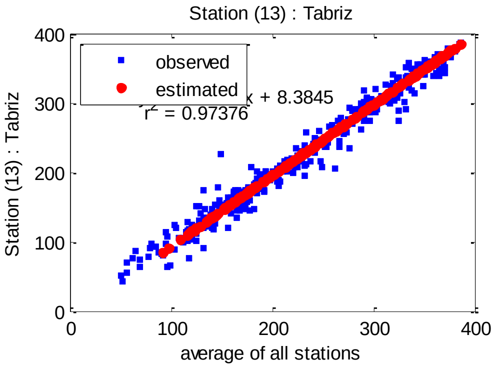
Station (13) : Tabriz
observed
estimated
+ 8.3845
r2 = 0.97376
Station (13) : Tabriz
average of all stations

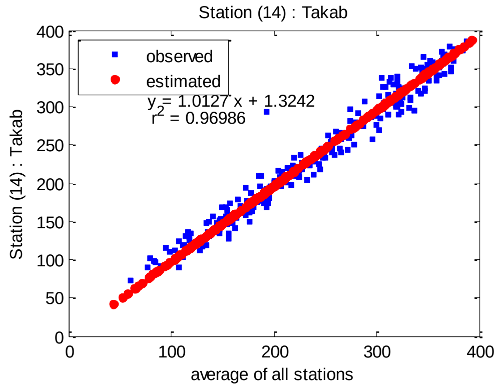
Station (14) : Takab
observed
estimated
y = 1.0127 x + 1.3242
r2 = 0.96986
Station (14) : Takab
average of all stations

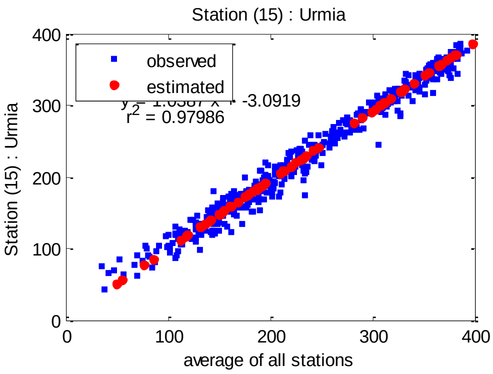
Station (15) : Urmia
observed
estimated
-3.0919
r2 = 0.97986
Station (15) : Urmia
average of all stations

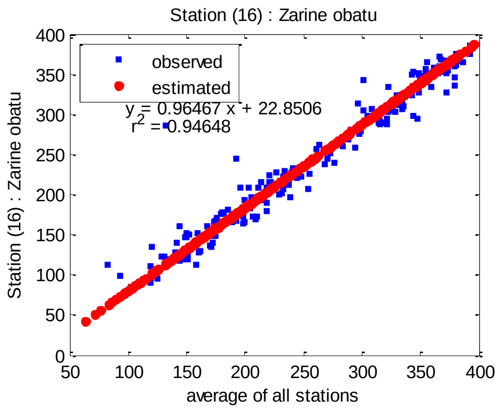
Station (16) : Zarine obatu
observed
estimated
y = 0.96467 x + 22.8506
r2 = 0.94648
Station (16) : Zarine obatu
average of all stations

C.5. Water Surface Temperature (WST) missing data

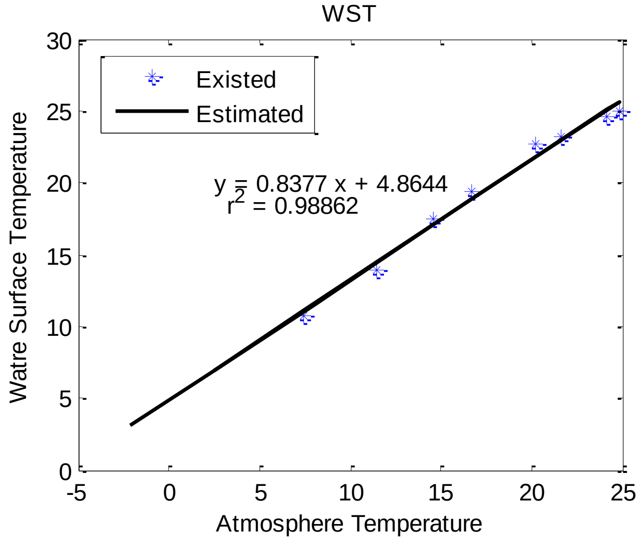

C.5. Pan Evaporation missing data and conversion to saline water evaporation